# Appendix A: Population viability analysis of *Pycnopodia helianthoides*

Nick Tolimieri

## Table of Contents

## A1 Prior Work

There are two prior assessments of *Pycnopodia helianthoides* status that investigate its response to sea star wasting syndrome (SSWS) and current status range-wide, from the Aleutian Islands to Baja California: Gravem et al. (2021, the IUCN Red List Report) and Hamilton et al. (2021).

In 2020, the IUCN conducted the first ever status assessment of *P. helianthoides* throughout its range (Gravem et al. 2021). Estimates of population size were based on mean density in various regions, as calculated from a suite of distinct sampling efforts, and the availability of habitat. The IUCN assessment concluded that the status of the sunflower sea star on a range-wide basis was Critically Endangered, citing a >90% loss in global abundance since 2013 (Gravem et al. 2021).

Additionally, Hamilton et al. (2021) used logistic models (general linear model with binomial errors and logit links) and presence-absence data to estimate the timing and the extent of the decline in occurrence among 12 regions. Overall, range-wide occurrence declined by 52.3%, with more severe declines of 92.2% in occurrence from Oregon southward. Where density data were available, Hamilton et al. (2021) also used zero-inflated generalized linear models (with Poisson errors and log-link) to estimate the change in density among regions and between phases (pre- and post-SSWS). Density declined by 99.2% from Baja California to the Washington coast, while declines were slightly lower (but greater than 87.8%) in regions from British Columbia through the Aleutian Islands, including the Salish Sea.

## A2 Present analysis

The population viability analysis (PVA) that follows uses multivariate autoregressive state space (MARSS) models (Holmes et al. 2012; Tolimieri et al. 2017; Holmes et al. 2021) to augment the above investigations by analyzing population trends of *P. helianthoides* prior to and following the onset of SSWS. MARSS models are a common form of count-based (or density-based) population viability analysis (PVA) and have a number of advantages. Importantly, one can estimate both population growth rate and separate process variance (real biological variation in population size around the longer-term abundance trend) from observation variance (due to sampling error). The estimates of population growth rate and process variance can then be used to calculate extinction risk – typically the probability that population size will drop below some threshold (Holmes et al. 2020). Additionally, MARSS is adept at handling multiple data sources and missing data, and incorporating space. The specifics of MARSS models are discussed below in more detail.

## A3 Data sources

As part of the IUCN status assessment process, Gravem et al. (2021) contacted a broad array of government, non-government, academic, and private data holders engaged in both direct and indirect monitoring of *P. helianthoides* occurrence, abundance, density, and habitat use throughout the range of the species. After careful evaluation of the temporal

span, accuracy, taxonomic resolution, and verifiability of this suite of data sources, they identified 31 data sets that met minimum criteria for use in describing abundance trends over time (their Figure A1 and Table A1).

The majority of data used here in the MARSS analyses were originally compiled by Hamilton et al. (2021) and Gravem et al. (2021). However, many of the time series in the IUCN data set contain only presence/absence data (Table AA3.1). For example, the trawl data from the Alaska Fisheries Science Center (AFSC_Trawl_AK) contain only presence/absence observations. These presence/absence data sets were not used for the present analyses.

The remaining data sets that contained density information were assessed for use in the MARSS analyses. The data sets were of varying temporal span and sampling frequency (Figure A3.1). Data sets with fewer than five (5) years of observations (Schultz_Dive_BC, NOAA_Dive_GlacierBay, Lee_Dive_BC, Kvitek_Dive_Olympic, Konar_Dive_Aleutians, CCIRA_Dive_BC) were eliminated from the analysis, as were two data sets that contained only pre-SSWS information from before the recent time period (Dean_Dive_PWS, Duggins_Dive_AK). One data set (NOAA_Trawl_ContigUSA) was removed and replaced with updated information obtained from the original data providers. See Northwest Fisheries Science Center's West Coast Groundfish Bottom Trawl Survey (WCGBTS) for more detail. Several new data sets were added, and these are discussed and summarized below.

While MARSS can use "gappy" data with missing observations and time series of different lengths, the data do need to be in a time-series format. For some data sets, the data were summarized to produce time series. For example, the NWFSC trawl data (WCGBTS), which come from a depth-stratified random sampling design, were averaged within latitude and depth bins for each year to create a times series for that bin. More detail follows below for each data source.

For data attributions and availability see Hamilton et al. (2021) and Gravem et al. (2021).

**Table A3.1.** Data sources from the IUCN Red List Report (Gravem et al. 2021) that do or do not contain density information.

| Time series | Density | Time series | Density |
|---|---|---|---|
| AFSC_Trawl_AK | N | MBNMS_Dive_BigSur | Y |
| CACS_Intertidal_AK | Y | NOAA_Dive_GlacierBay | Y |
| CADFW_Dive_NorCal | Y | NOAA_Trawl_ContigUSA | Y |
| CADFW_ROV_CA | Y | OceanWise_CitSciDive_BC | N |
| CCIRA_Dive_BC | Y | OCNMS_Dive_Olympic | Y |
| COBI_Dive_Baja | Y | ODFW_Dive_OR | Y |
| Dean_Dive_PWS | Y | ODFW_ROV_OR | Y |
| Duggins_Dive_AK | Y | ParksCanada_Dive_Haida | Y |
| Hakai_Dive_BC | Y | PISCO_Dive_CA | Y |
| iNaturalist_CitSciObs_Global | N | REEF_Dive_Namerica | N |
| Konar_Dive_Aleutians | Y | ReefCheck_Dive_CA | Y |
| Konar_Intertidal_AK | Y | Salomon_Dive_HaidaGwaii | Y |
| Kroeker_Dive_Sitka | Y | Schultz_Dive_BC | Y |
| Kvitek_Dive_Olympic | Y | UABC_Dive_Baja | Y |
| Lee_Dive_BC | Y | Watson_Dive_Vanls | Y |
| MARINe_CitSciDive_AK-BC | Y | WDFW bottom trawl survey | Y |
| MARINe_CitSciObs_Global | N | WDFWShellfish_Dive_WA | Y |

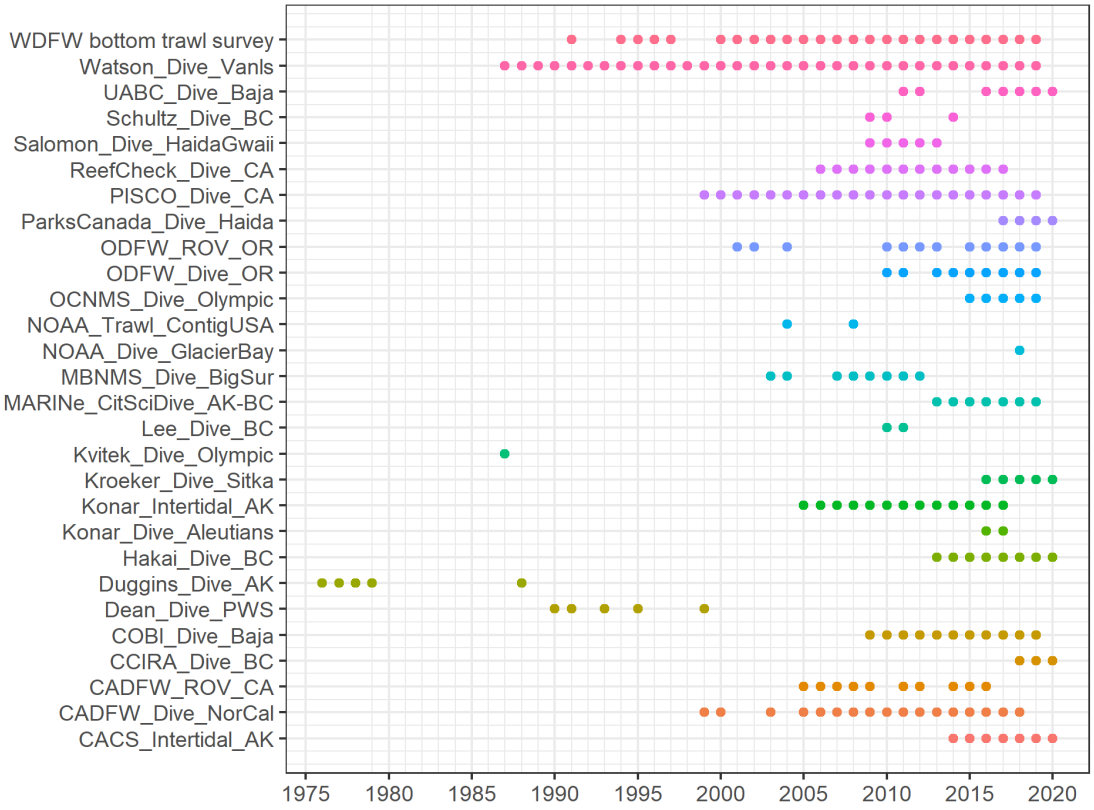


**Figure A3.1.** Availability of density estimates through time for the times series included in the IUCN data set. The data have been filtered to show only those data sources with density estimates. Not all these data sets were used in the MARSS analyses.

## A3.1 Center for Alaskan Coastal Studies intertidal data (CACS_Intertidal_AK)

These data (CACS_Intertidal_AK) contain time series for four locations near Homer, AK, and Kachemak Bay State Park in the western edge of the east Gulf of Alaska region, with multiple samples per year (Figure A3.2). The data run from 2014-20. Data were summarized by location (unique latitude and longitude) and year by summing all *P. helianthoides* observations within a location and year and dividing by the total area sampled.

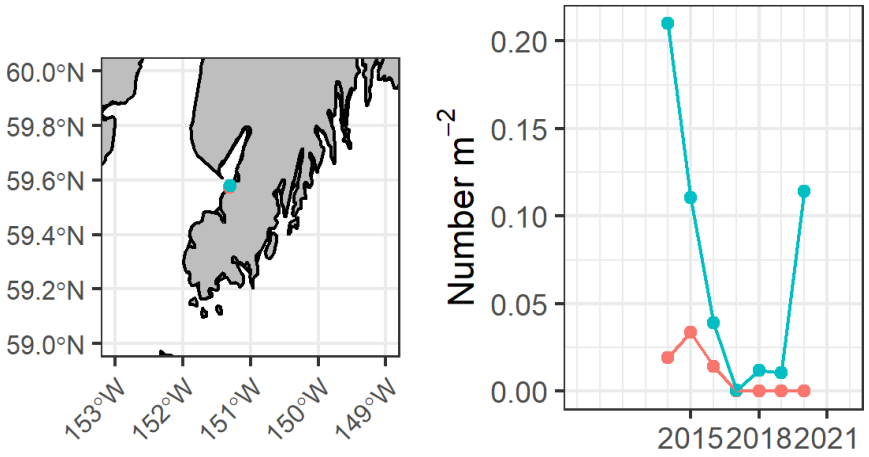


**Figure A3.2.** Location and time series of the CACS Intertidal data for Alaska. Note the two locations are located close together and their points overlap on the figure.

## A3.2 California Department of Fish and Wildlife dive data for northern California (CADFW_Dive_NorCal)

The California Department of Fish and Wildlife dive surveys (CADFW_Dive_NorCal) contain information for 12 sites located north of San Francisco Bay from 1999-2018 (Figure A3.3). Data were summarized by site and year by summing all *P. helianthoides* observations for a site in a given year and dividing by the total area. The number of years sampled per site varied between one and eight. These data show a strong increase in density of *P. helianthoides* prior to 2013, followed by an equally extreme collapse well below previous low densities observed earlier in the time series. No *P. helianthoides* were observed in 2017 or 2018.

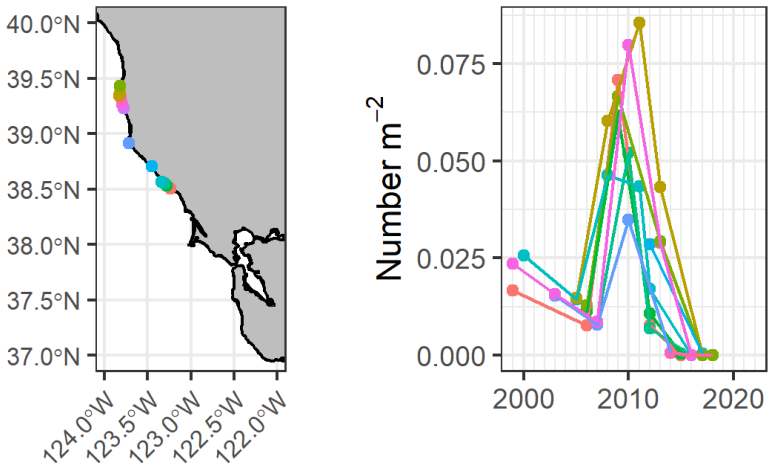


**Figure A3.3.** Location and time series CADFW dive surveys and time series of *P. helianthoides* density.

## A3.3 California Department of Fish and Wildlife ROV surveys (CADFW_ROV_CA)

The California Department of Fish and Wildlife ROV data (CADFW_ROV_CA) cover most of the California coast from 32.6-41.9 °N for 2005-2016 at depth between 17.4-348.4 m and include a total of 266 observations (Figure A3.4).

The exact location of trawls varies somewhat from year to year. To create a time series, data were summarized by latitude bin (rounding down to the nearest degree latitude). There were five observations shallower than 5 m, which were excluded from the analyses because they did not form a time series. These data are shown in Figure A3.4, but only the deep data were used in the MARSS analysis.

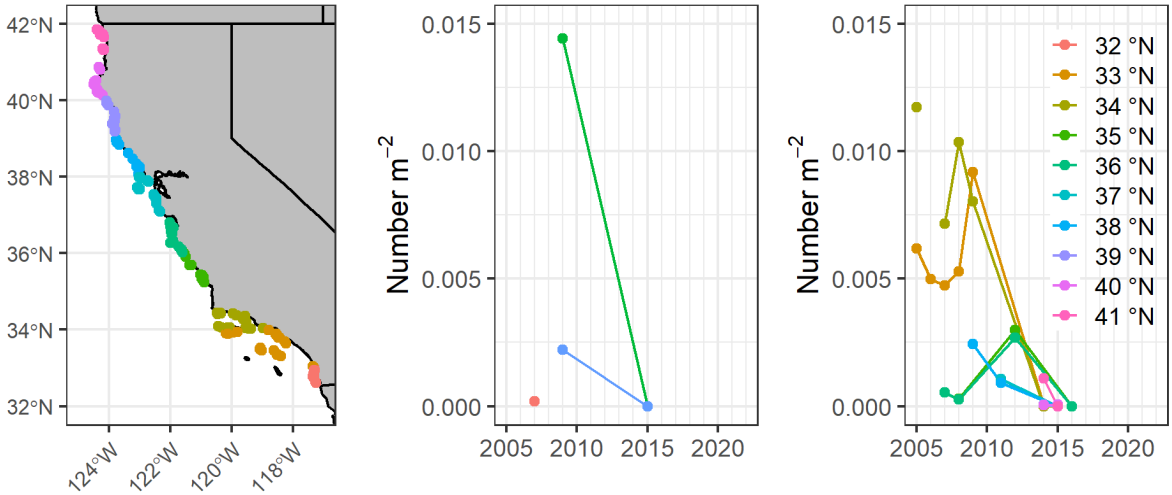


**Figure A3.4.** Location and time series of the California Department of Fish and Wildlife ROV data. The middle pane shows data for areas <25 m. The right pane shows data for surveys in >25 m depth.

## A3.4 Comunidad y Biodiversidad dive data for Baja (COBI_Dive_Baja)

The Comunidad y Biodiversidad dive data for Baja California (COBI_Dive_Baja) contain information on 14 locations from 2009-19 (Figure A3.5). Data were summarized by year

and site by dividing the total number of *P. helianthoides* observed by the total area sampled. The more northern sampling locations had higher densities in 2013 than did the more southern areas: however, all rapidly declined after 2013.

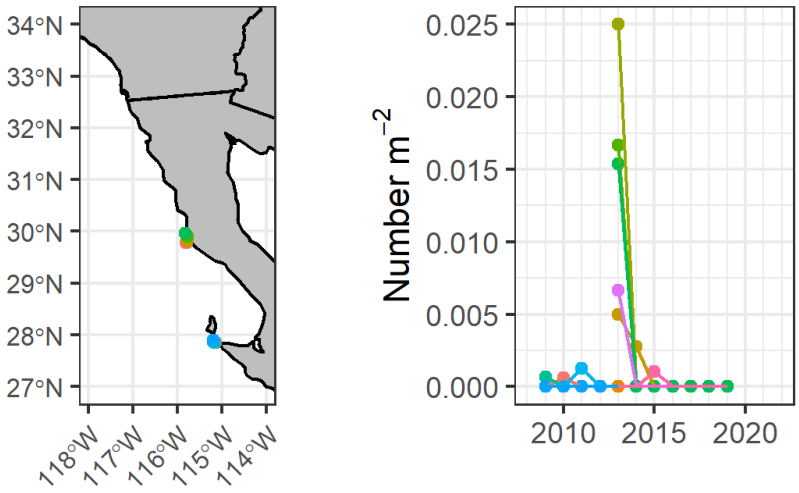


**Figure A3.5.** Location and time series of the COBI dive surveys in Baja California.

## A3.5 Cote dive surveys (Cote_Dive)

The data from Dr. Isabelle Cote at Simon Fraser University cover sites in the Salish Sea and in coastal British Columbia (Figure A3.6). The data have no area measurements and are averaged counts. For MARSS analyses, this is not a huge problem as the data can be treated as independent time series from other density data and combined or not combined based on model testing results. The data run from 2007-21 and cover nine sites. These data were not included in the IUCN assessment and enrich analysis of *P. helianthoides* population trends in British Columbia.

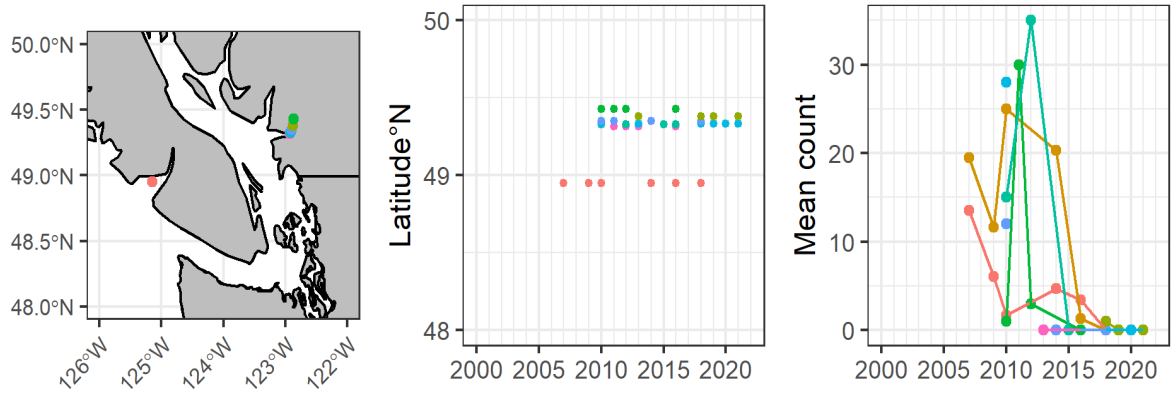


**Figure A3.6.** Locations and time series of data provided by Isabelle Cote from Simon Fraser University. Middle pane shows the latitudinal range and frequency of sampling by time series. Right pane showed the time series.

## A3.6 Derelict gear survey (Derelict_Gear_WA)

The Northwest Straits Foundation manages the Washington State Derelict Fishing Gear Database (Derelict_Gear_WA). *Pycnopodia helianthoides* are observed on derelict fishing

gear in the Salish Sea during gear retrieval/cleanup (Table AA3.2, Figure A3.7). Data exist for 2004-22. Data were binned into nine sub-regions to create time series by averaging the number of *P. helianthoides* observed with each retrieval. While there are multiple gear types within the data set, data were averaged by major basin or feature and gear type was ignored. These data were not included in the IUCN assessment and enrich analysis of *P. helianthoides* population trends in the Salish Sea.

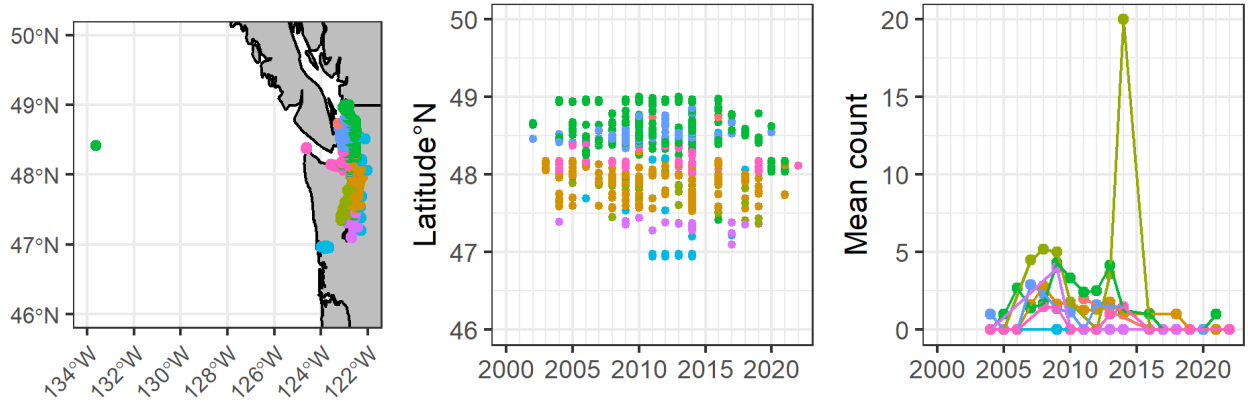


**Figure A3.7.** Location, data availability, and time series of *P. helianthoides* retrieved along with derelict gear in the Salish Sea.

**Table A3.2.** Subregions used to calculate mean *P. helianthoides* counts for the derelict fishing gear survey. Data for British Columbia and the Pacific Coast were not included in the MARSS analysis.

| Subregion | Samples |
|---|---|
| British Columbia | 2 |
| Central Puget Sound | 3,196 |
| Hood Canal | 117 |
| North Puget Sound | 4,236 |
| Pacific Coast | 1 |
| Rivers/Lakes | 174 |
| San Juan Islands | 2,192 |
| South Puget Sound | 33 |
| Strait of Juan de Fuca | 1,389 |

## A3.7 Elwha nearshore dive surveys (Elwha nearshore)

The U.S. Geological Survey conducts nearshore dive surveys in the vicinity of the mouth of the Elwha River, WA, which empties into the Strait of Juan de Fuca (Figure A3.8). The data cover 17 sites from 2008-21. These data were not included in the IUCN assessment and are used without modification, as individual sites were re-sampled over time. The file provided by the U.S. Geological Survey did not contain specific latitude and longitude information.

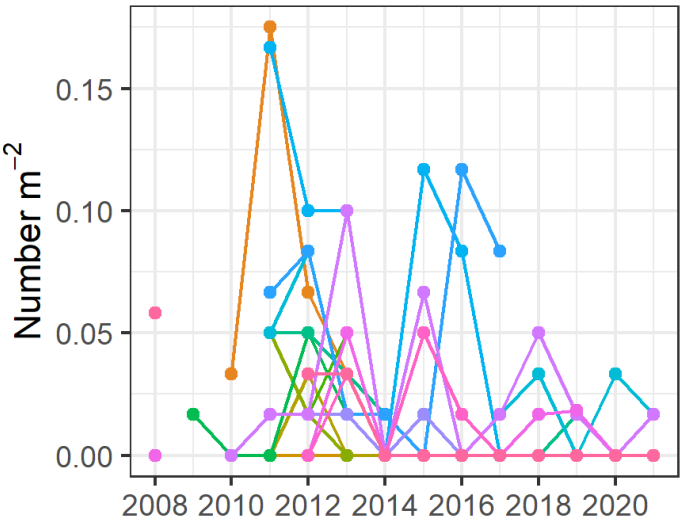


**Figure A3.8.** Time series of *P. helianthoides* density from sites near the Elwha River.

## A3.8 Hakai Institute dive survey data, British Columbia (Hakai_Dive_BC)

The Hakai Institute dive data for British Columbia (Hakai_Dive_BC) contain information on 148 sites from 2013-20 (Figure A3.9). However, many of the specific latitude and longitude locations were sampled only once, but were often quite close together. Therefore, we summarized the Hakai Institute data by binning observations into 0.1 °N latitude bins and then calculating the mean density as the total number of *P. helianthoides* observed divided by the total area sample for a given bin and year. This approach produced seven time series. Two sites had positive observations of *P. helianthoides* in 2020.

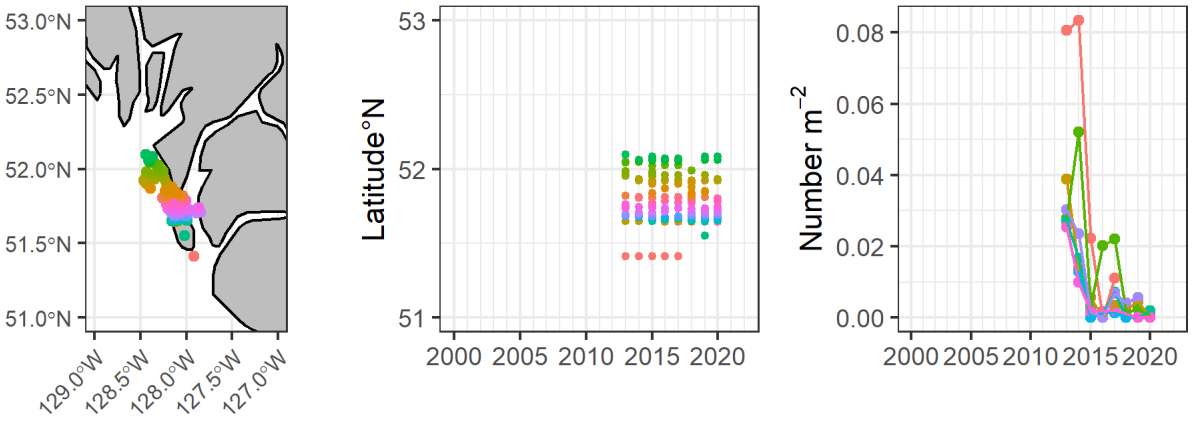


**Figure A3.9.** Location, data availability, and time series of dive observation from the Hakai Institute data set. Note that for the right-hand pane, data have been summarized by 0.1 degree latitude bins.

## A3.9 Konar intertidal data for Alaska (Konar_Intertidal_AK)

The Konar intertidal (Konar_Intertidal_AK) data contain observations at 30 sites from 2005-17 (Figure A3.10). The data include time series with annual assessments for multiple sites and were used without modification.

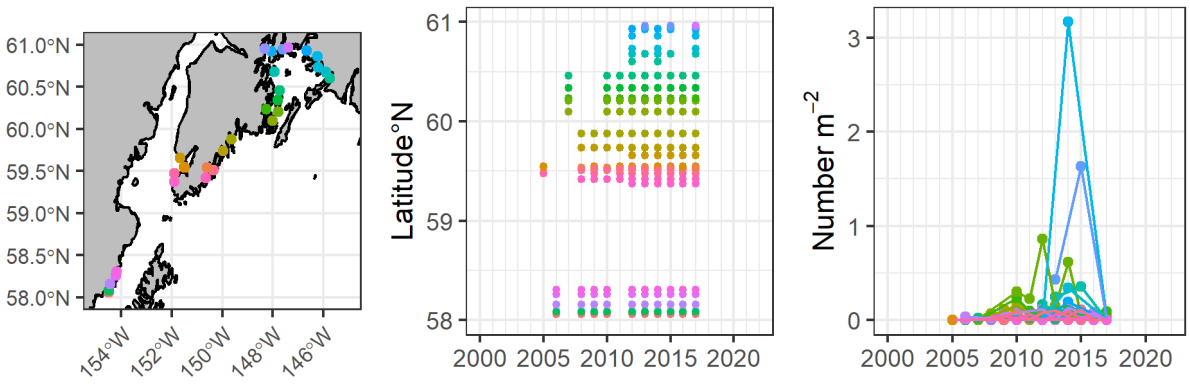


**Figure A3.10.** Location, data availability, and time series of abundance for the Konar intertidal observations.

## A3.10 Kroeker dive surveys for Sitka, AK (Kroeker_Dive_Sitka)

The Kroeker dive data from the University of California Santa Cruz for the Sitka, AK area (Kroeker_Dive_Sitka) contain observations at four sites from 2016-20 (Figure A3.11). As there were multiple surveys at a site in a given year (often two), data were summarized by year and site by summing the total number of observed *P. helianthoides* and dividing by the total area sampled.

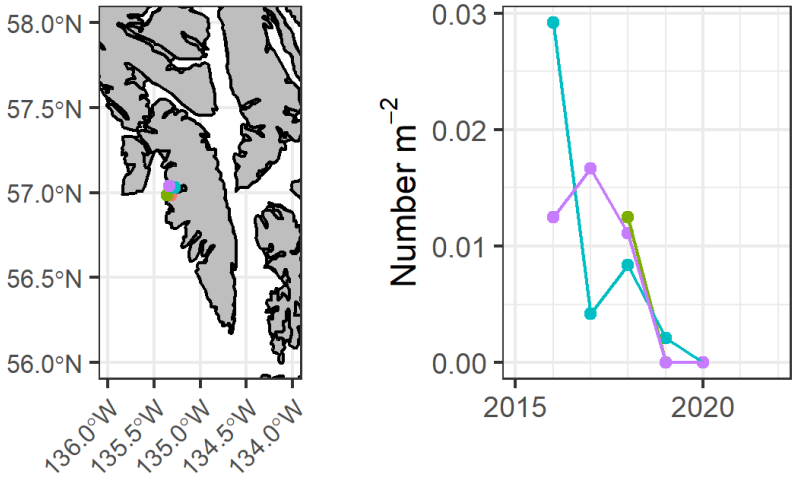


**Figure A3.11.** Location and time series for the Kroeker dive survey data.

## A3.11 Multi-Agency Rocky Intertidal Network, Alaska and British Columbia (MARINe_CitSciDive_AK-BC)

The Multi-Agency Rocky Intertidal Network Citizen Science dive data for Alaska and British Columbia (MARINe_CitSciDive_AK-BC) contain information on 19 sites from 2013-19 (Figure A3.12). Because there were often more than one set of observations per year, data were summarized by year and site by dividing the total *P. helianthoides* observed by the total area sampled. This data set primarily provides information for the Salish Sea as many of the other sites were eventually deleted because the site-level time series were short.

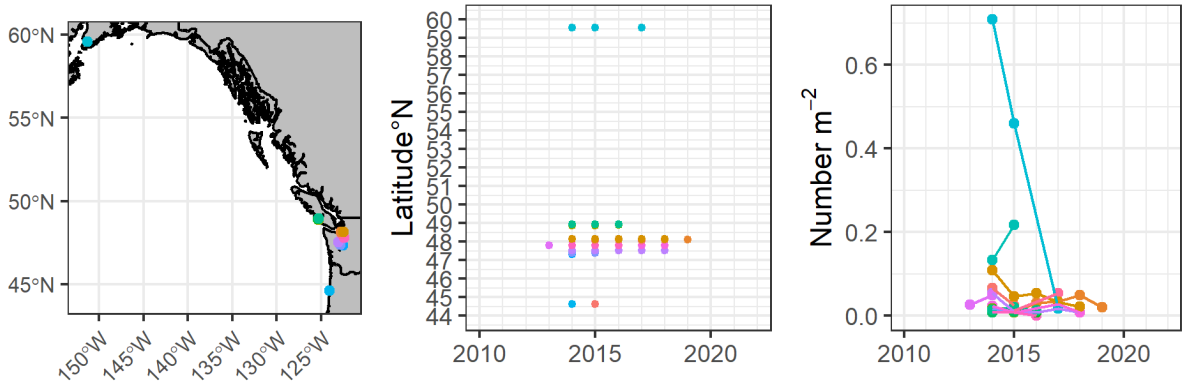


**Figure A3.12.** MARINe Citizen Science Dive data for Alaska and British Columbia.

## A3.12 Monterey Bay National Marine Sanctuary (MBNMS) dive surveys, Big Sur (MBNMS_Dive_BigSur)

The Monterey Bay National Marine Sanctuary dive data for Big Sur (MBNMS_Dive_BigSur) contain information on 68 locations from 2003-12 (Figure A3.12). Data were binned by 0.1 degree latitude bins by dividing the total *P. helianthoides* observed by the total area sampled. Even though this data set contains no post-SSWS information, the data provide trend information just prior to the onset of SSWS and were retained.

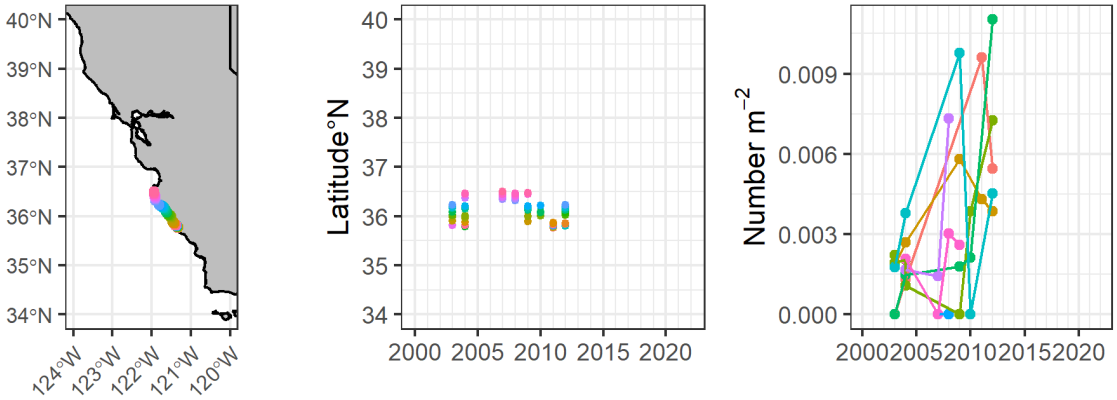


**Figure A3.13.** Location, data availability, and time series of abundance for the MBNMS dive survey data.

## A3.13 Northwest Fisheries Science Center's West Coast Groundfish Bottom Trawl Survey (WCGBTS)

In the Hamilton and IUCN analyses (Gravem et al. 2021; Hamilton et al. 2021), the West Coast Groundfish Bottom Trawl Survey (WCGBTS) (NOAA_Trawl_ContigUSA in Figure A3.1 of Gravem et al. 2021) contains observations for only 2004 and 2008, but the WCGBTS recorded density and biomass observations for *P. helianthoides* from 2003-21 (excluding 2020). For this MARSS analysis, the limited NOAA_Trawl_ContigUSA data set was removed and replaced with the complete WCGBTS data. The WCGBTS data are available from: https://www.webapps.nwfsc.noaa.gov/data/map.

The Northwest Fisheries Science Center (NWFSC) conducts the WCGBTS annually (Keller et al. 2017). The survey follows a depth-stratified random sampling design. The trawl data span 32-48.5 degrees latitude, and cover 36-1285 m in depth. Data were available for 2003-21 and contain 11,422 trawls (after removing trawls with unacceptable performance, aka water hauls, and trawls conducted in areas that were eventually closed to trawling, e.g., cowcod and rockfish closed areas). *Pycnopodia helianthoides* was observed in 1046 of these samples. All positive hauls contain biomass data (kg per hectare), but count/density were available for slightly fewer (n = 946). The survey observed a total of 2625 *P. helianthoides*, although this is an under-count given the discrepancy between total samples with biomass and total samples with positive counts.

While there is some variation with latitude, the majority of hauls with *P. helianthoides* were from waters less than 250 m (Figure A3.14).

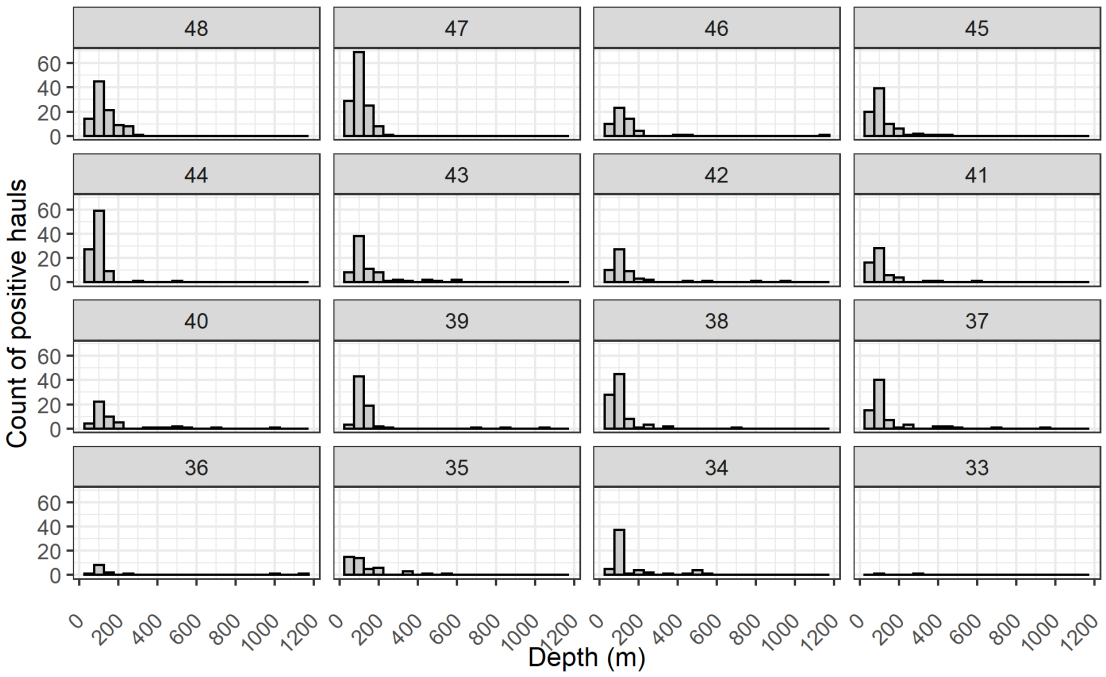


**Figure A3.14.** Depth distribution of positive hauls across latitude bins and depth bins. Latitude was rounded to the nearest degree; depth was rounded to the nearest 100 m contour.

*Pycnopodia helianthoides* density was not particularly high in the trawl survey compared to shallower dive surveys; however, the density trends were similar. Density peaked in 2013, declined suddenly in 2014, and went to essentially zero in 2015 with no sign of recovery (Figure A3.15). The survey recorded 2618 *P. helianthoides* from 2003-14 but only seven individuals from 2015-21.

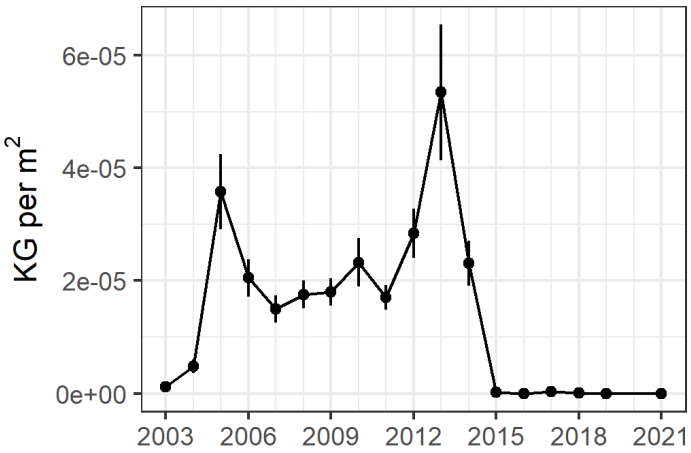


**Figure A3.15.** Mean density of *P. helianthoides* within the WCGBTS across all latitudes and depths and from 2003-21. Error bars indicate 1.0 se.

To create time series for the MARSS analysis, we summarized the WCGBTS by depth and latitude bins. We used two depth bins (<250 m and >250 m) based on the distribution of positive occurrence in Figure A3.14. For latitude we first binned samples by the five West Coast regions used by Hamilton et al (2021): Washington, Oregon, Northern California, Central California, and Southern California. In order to capture additional variation, we then subdivided these bins into three evenly wide (within each region) latitude bins (1-3). We then calculated the mean density $m^{-2}$ for each bin and year combination by summing the total count across all hauls and dividing by the total haul area. Densities were clearly higher in the shallow trawl depth bin and variable in general until 2015, after which there are very few density observations above zero individual per $m^2$ (Figure A3.16). Data deeper than 250 m were excluded from the MARSS analysis because there were very few observations of *P. helianthoides*.

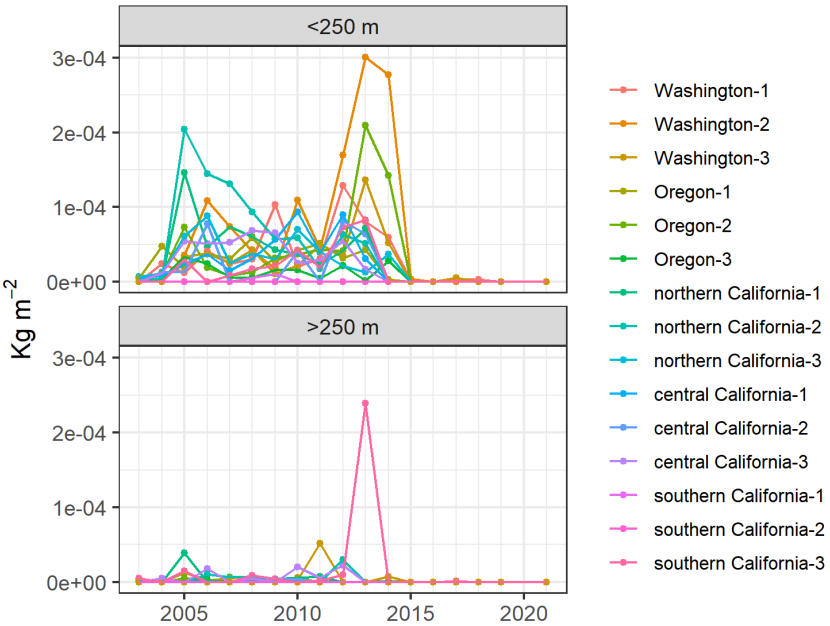


**Figure A3.16.** Mean density of *P. helianthoides* summarized by depth and latitude bins for inclusion in the MARSS analysis.

## A3.14 NWFSC Olympic Coast Dive Data (OCNMS_Dive_Olympic)

Dive teams from NOAA's Northwest Fisheries Science Center (NWFSC) and the National Marine Sanctuaries (NMS) have conducted surveys along the Olympic Coast since 2015, excluding 2020 due to COVID restrictions (Figure A3.17). These data were included in Hamilton et al. (2021) and the IUCN report (Gravem et al. 2021) but are updated here to include data for 2021.

Data were initially summarized by site and year (as in Hamilton et al. [2021]) by summing all *P. helianthoides* counts per site and dividing by the total area surveyed. *Pycnopodia helianthoides* were rare on these surveys, occurring in small numbers at different sites in different years. Therefore, the five sites were averaged to obtain a single time series for the Olympic Coast data by summing the number of individuals observed in a year and dividing by the total area searched.

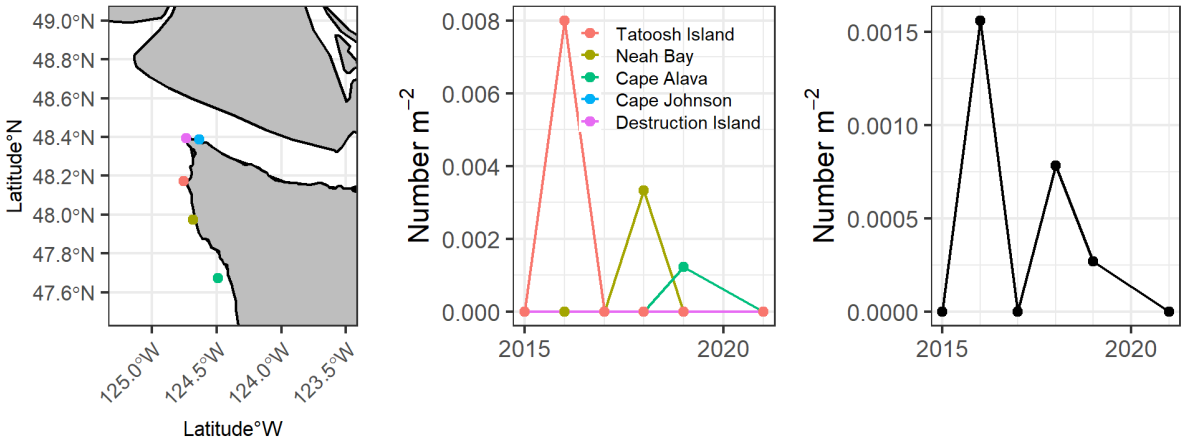


**Figure A3.17.** Location and time series of *P. helianthoides* at five sites along the Olympic Coast of Washington from 2015-2021. The right pane shows the summarized data used in the MARSS analysis.

## A3.15 Oregon Department of Fish and Wildlife dive data (ODFW_Dive_OR)

The Oregon Department of Fish and Wildlife dive data (ODFW_Dive_OR) contain observations from 2010-19 for 10 sites along the Oregon coast (Figure A3.18). These sites were included in the MARSS analysis. However, it is clear that in all cases, *P. helianthoides* density went to zero observed individuals by 2017 (Figure A3.18). Interestingly, at several sites declines began as early as 2011.

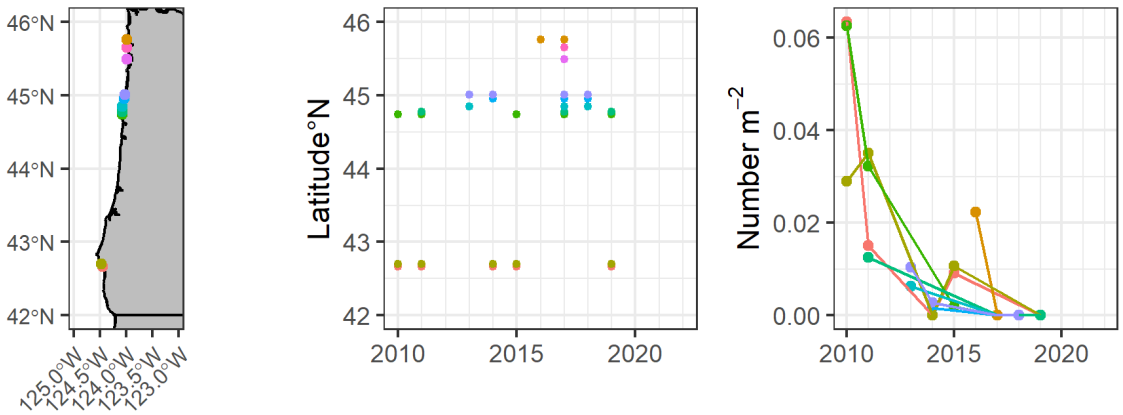


**Figure A3.18.** Location, data availability, and time series of dive survey data off of Oregon by ODFW.

## A3.16 Oregon Department of Fish and Wildlife Remotely Operated Vehicle survey (ODFW_ROV_OR)

The Oregon Department of Fish and Wildlife supplied data from Remotely Operated Vehicle surveys (ODFW_ROV_OR) conducted from 2001-19. The data are a relative index of counts per 100-m transects and not an actual density estimate. The data cover six regions of the Oregon coast (Figure A3.19). Data were summarized by Oregon region (location) since many individual sites were sampled only once or twice across the time series. Likewise, there were both shallow (< 25m) and deep (>25 m) transects, but the shallow transects were dropped because the time series were too short. The resulting index is the number of *P. helianthoides* observed per 100 m, representing a single ROV transect. These data were not included in the IUCN analyses (no specific density estimates) (Gravem et al. 2021).

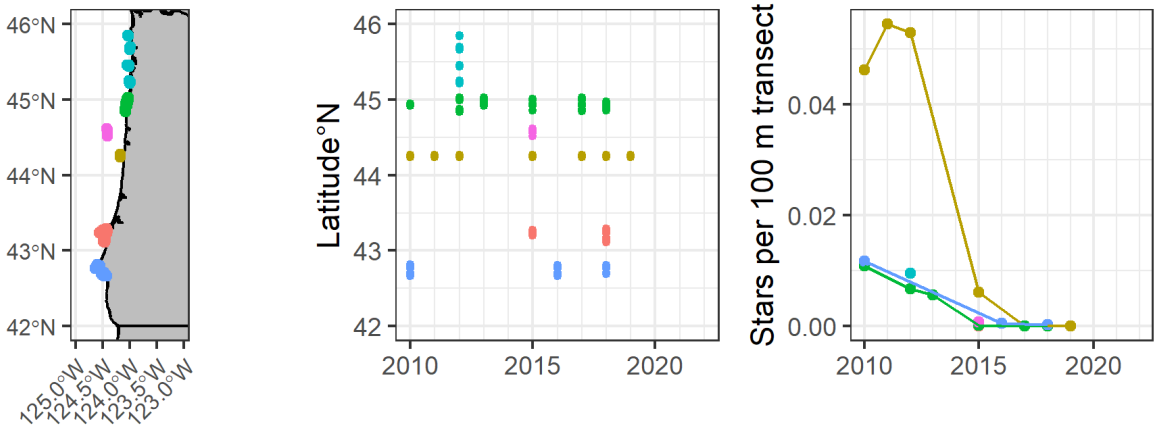


**Figure A3.19.** Location, data availability, and time series of ROV survey data off of Oregon by ODFW.

## A3.17 Parks Canada dive data for Haida (ParksCanada_Dive_Haida)

Dive data from Parks Canada (ParksCanada_Dive_Haida) include two sites in Gwaii Haanas National Park Reserve and Haida Heritage Site (Figure A3.20). The data cover from 2017-20. These data were used directly and not summarized. Note, however, there were only four years of data, and this data set was eventually excluded from the MARSS analysis.

Regardless, the data show the same trend as other locations with *P. helianthoides* density dropping to zero individuals per m$^2$ by 2019.

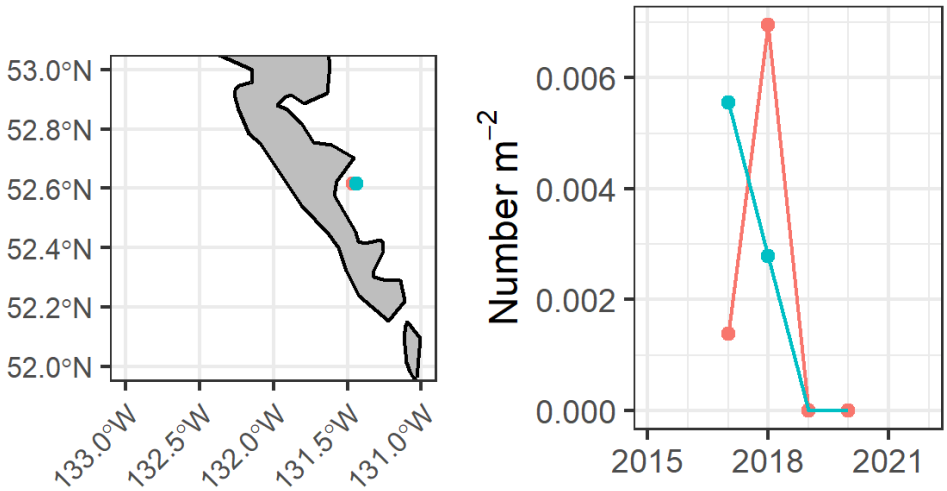


**Figure A3.20.** Data from Parks Canada for Haida Gwaii.

## A3.18 Partnership for Interdisciplinary Studies of Coastal Oceans (PISCO) dive data (PISCO_Dive_CA)

PISCO dive data (PISCO_Dive_CA) cover 280 locations (unique latitude and longitude combinations), primarily in central and southern California (Figure A3.21). While there are data north of Point Arena (39 °N), these data pertain only to the pre-SSWS period (Figure A3.21) and, thus, could not be used to inform changes in population trend before and after the pandemic.

Data were summarized by "location" (latitude/longitude) by year to obtain a yearly average. For each location, counts and area from individual surveys were summed within a year, and total annual count was divided by total annual area surveyed to obtain a yearly mean density. While density was highly variable, observations went to essentially zero by 2019.

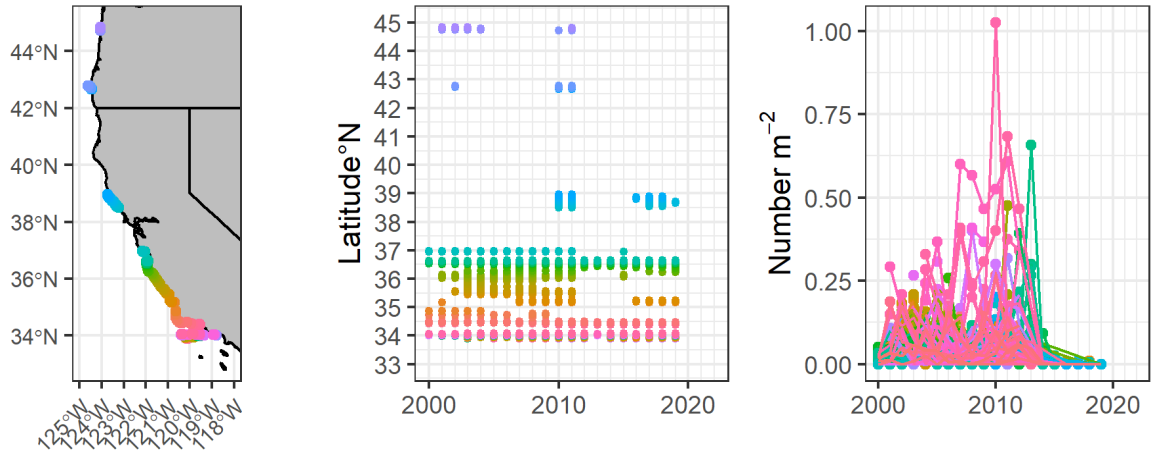


**Figure A3.21.** Location, availability, and time series of PISCO dive data.

## A3.19 Reef Check California dive data (ReefCheck_Dive_CA)

The Reef Check data (ReefCheck_Dive_CA) span most of the California coast, run from 2006-17, and cover 121 total sites from 32.7-42 °N (Figure A3.22). There are often multiple observations per year, usually in June and October. Data were summarized by year and site by summing all *P. helianthoides* observations and dividing by the total area.

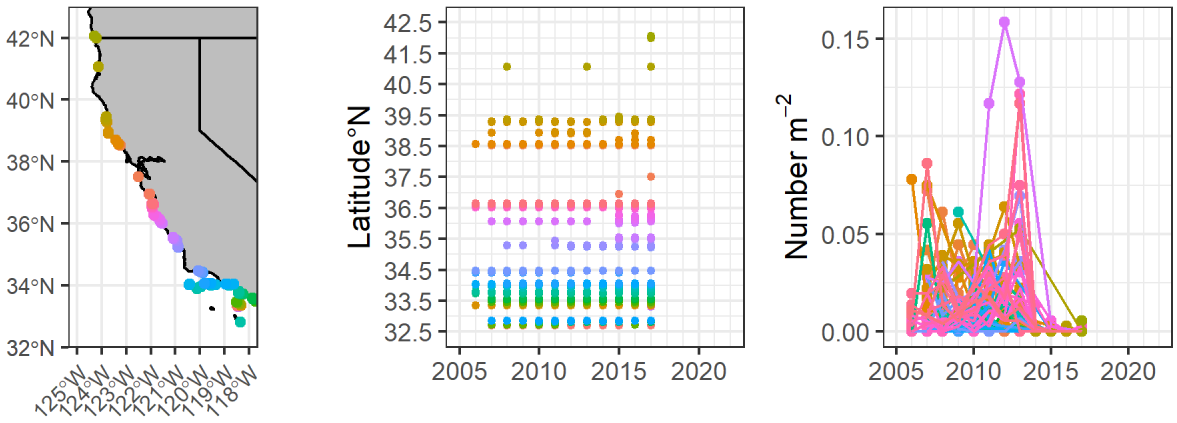


**Figure A3.22.** Location, availability, and time series of Reef Check California dive data.

## A3.20 Reef Environmental Education Foundation surveys (REEF)

Hamilton et al. (2021) used presence/absence data from the Reef Environmental Education Foundation (REEF) dive surveys. In the context of their analyses, this decision makes sense because they compared either presence/absence or density, and for the density analyses they needed numbers per m$^2$. However, MARSS can incorporate multiple data types into a single analysis, which gives the present analysis more flexibility to include the complete REEF data set (discussed in detail below). The REEF data are not counts or density data but a ranked abundance (without area estimates) from 0-4: None = 0, **S**ingle=1, **F**ew=2-10, **M**any=11-100, and **A**bundant=over 100 (or, 0 = 0, 1 = 1, 2 = 2-10, 3 = 11-100, and 4 = 101+). These pseudo-abundance values were used here and have been used in a similar manner in the past to successfully model population trends in other species (Tolimieri et al. 2017).

Observations from Southern California to British Columbia, including the Salish Sea, are used here. There were only 17 observations in two years (2013 & 2014) from Alaska, and these were excluded due to the shortness of the times series. The data file provided contained no data for Northern California. REEF data were provided by Dan Greenberg (REEF 2022).

The raw REEF data were converted to an abundance index. First, the Density Index was calculated:

$$Den = \big((nS * 1) + (nF * 2) + (nM * 3) + (nA * 4)\big)/N$$

where n is the number of surveys where *P. helianthoides* were **S**ingle, **F**ew, **M**any, or **A**bundant, and N is the total number of surveys reporting *P. helianthoides*.

We next determine the Sighting Frequency (SF) as:

$$SF = N_p/N_t$$

where $N_p$ is the number of surveys with *P. helianthoides* and $N_t$ is the total number of surveys. Den and SF are then multiplied to create an abundance index for each survey location ($ Abund = Den*DF$).

The REEF data have several levels of geographic information. Data are categorized by region ("geogr1" within the data file, e.g., Washington, southern California), subregion ("geogr2", e.g., basins within the Salish Sea), area ("geogr4", e.g., Santa Barbara and southern Channel Islands), and individual site ("geogr"). For most localities, data were summarized by area (Table A3.3) to help create longer, more complete time series. Because there were many areas in the Salish Sea compared to other regions (US and Canadian waters), we substitute subregion for area for samples from the Salish Sea (based on the first two digits in the REEF data "geogr" field).

**Table A3.3.** Availability of REEF dive survey data by Region (geogr1) and Area (geogr4). While listed separately here, the two Salish Sea regions were combined for the MARSS analysis.

| Region | Subregions | Areas | Sites | Dives |
|---|---|---|---|---|
| British Columbia | 1 | 2 | 17 | 684 |
| Oregon | 4 | 6 | 17 | 737 |
| Salish Sea Canada | 3 | 26 | 134 | 4,230 |
| Salish Sea USA | 7 | 28 | 203 | 16,569 |
| southern California | 2 | 4 | 38 | 2,799 |
| Washington | 1 | 1 | 1 | 90 |

After converting the Density index (Dens) and Sighting frequency (SF) for each REEF site to the Abundance Index, we summarized the Abundance Index by its level-4 geographic classification ("geogr4", Figure A3.23).

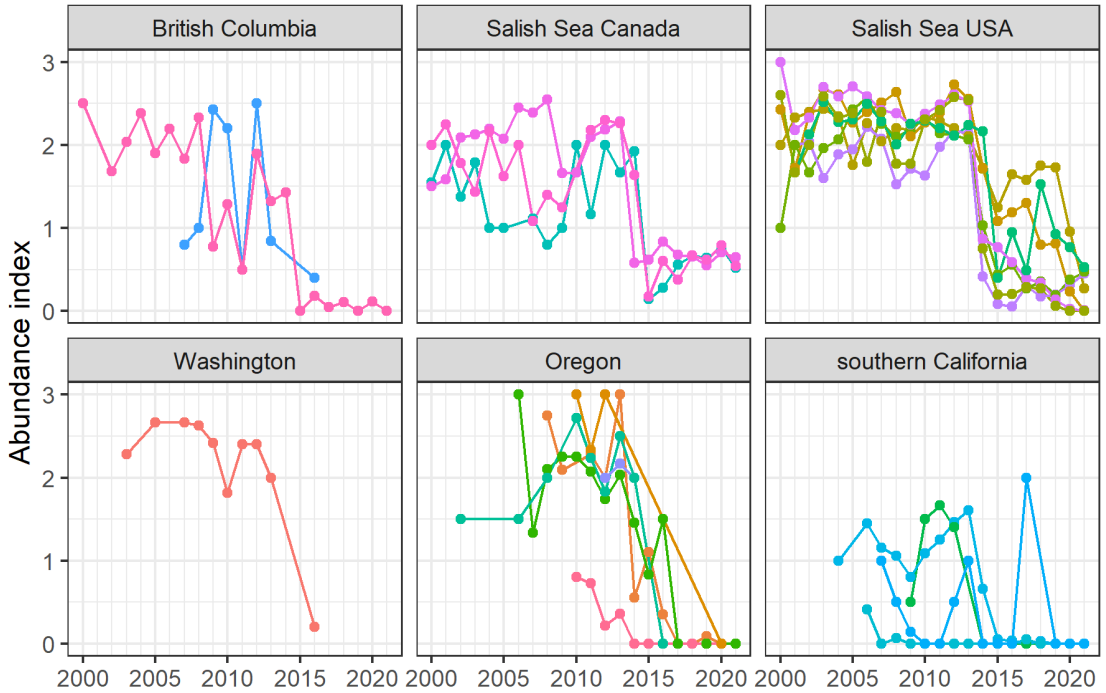


**Figure A3.23.** REEF abundance index summarized by area (geogr4). Note, while presented separately here, data for the two Salish Sea regions were combined in the MARSS analysis.

## A3.21 Salomon dive for Haida Gwaii (Salomon_Dive_HaidaGwaii)

Dive data from Dr. Anne Salomon at Simon Fraser University for Haida Gwaii (Salomon_Dive_HaidaGwaii) University contain information on 13 locations for 2009-13 (Figure A3.24). These data do not cross the ~2013 initiation of SSWS, but provide complementary pre-collapse information to the Parks Canada dive data for the Haida Gwaii area just prior to the onset of SSWS.

The Salomon data were summarized by year and site by summing total *P. helianthoides* observations and dividing by total area sampled. Sites with fewer than five years of data were removed for the MARSS analysis, leaving a total of six sites for analysis.

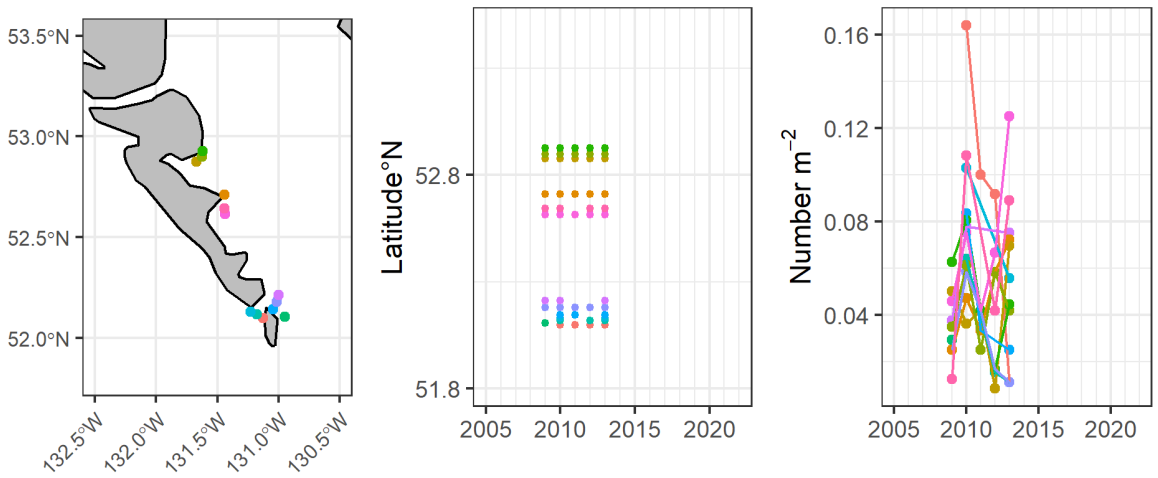


**Figure A3.24.** Sampling locations and times series for the Salomon dive data from Haida Gwaii.

## A3.22 Universidad Autonoma de Baja California dive surveys (UABC_Dive_Baja)

Dive data provided by the Universidad Autonoma de Baja California (UABC_Dive_Baja) contain information on 53 locations from 2011-20 (Figure A3.25). No sites (unique latitude and longitude combinations) had more than three years of observations. Therefore, data were combined by latitude bins (rounded down to the nearest latitude) to create more complete time series. Data were summarized by year and site (latitude bin) by dividing the total number of *P. helianthoides* observed by the total area sampled. The 31 °N bin was the only one containing both non-zero observations and a time series of reasonable length (Figure A3.25), and only this time series is included in the MARSS analysis.

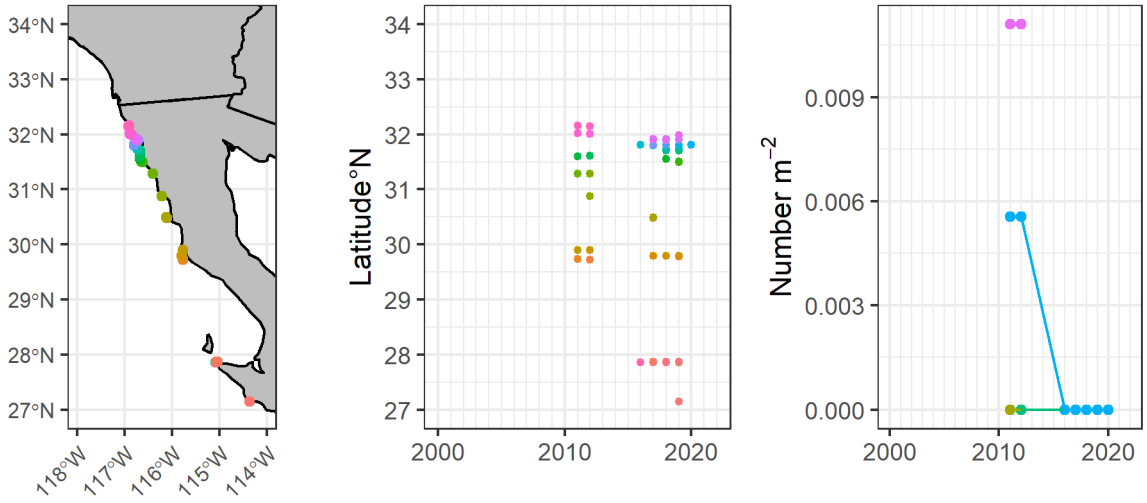


**Figure A3.25.** Location, data availability, and time series of the UABC Dive in Baja.

## A3.23 Washington Department of Fish and Wildlife (WDFW) bottom trawl survey, Salish Sea (WDFW_Trawl_WA)

Trawl survey data from the Washington Department of Fish and Wildlife (WDFW_Trawl_WA) run from 1991-21 and cover five sub-basins (defined as nine survey

regions that shift over the course of the time series) in two depth bins (<25 m, >25 m) within the US portion of the Salish Sea (Puget Sound, and the Strait of Juan de Fuca). Data were summarized by basin by dividing the total *P. helianthoides* observed by the total area trawled (Figures A3.26 and 3.27). Both strata showed strong increases in *P. helianthoides* densities from the 1990s through approximately 2010, followed by declines, and then drops to near zero densities, following the onset of SSWS.

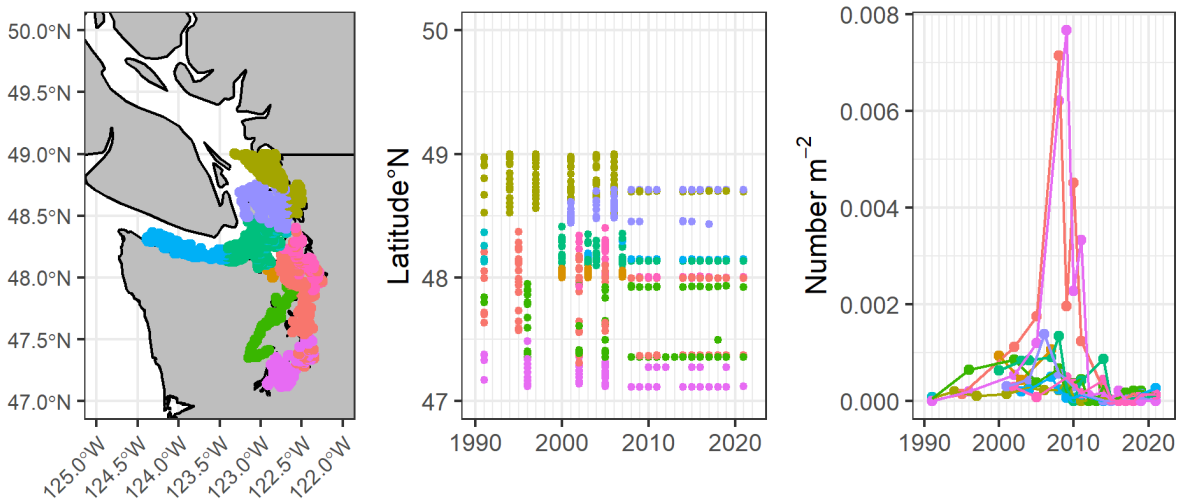


**Figure A3.26.** Location, data availability, and time series of *P. helianthoides* in the shallow stratum (> 25 m) of the WDFW trawl survey.

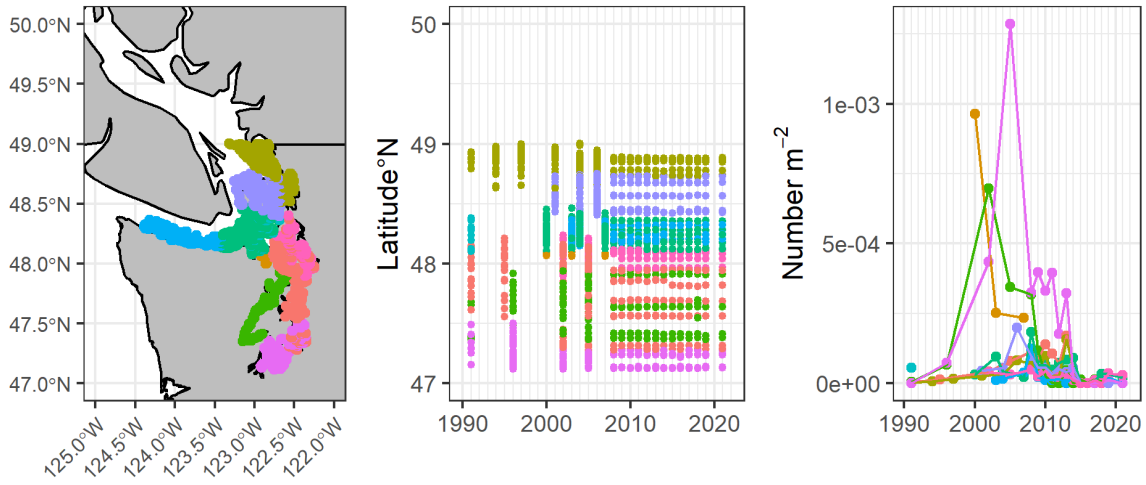


**Figure A3.27.** Location, data availability, and time series of *P. helianthoides* in the deep stratum (> 25 m) of the WDFW trawl survey.

## A3.24 WDFW shrimp test-fishery (WDFW_shrimp)

In the WDFW shrimp test-fishery (WDFW_shrimp), there are *P. helianthoides* observations running from 1987-2021 (Figure A3.28). The data are not density data but instead counts per soak time in hours. The test fishery operated in 627 locations. Time series of mean *P. helianthoides* observed per hour of soak time were calculated by summing the total number

of individuals observed in a location and dividing by the total number of hours soaked. These data were not included in the IUCN assessment (Gravem et al. 2021).

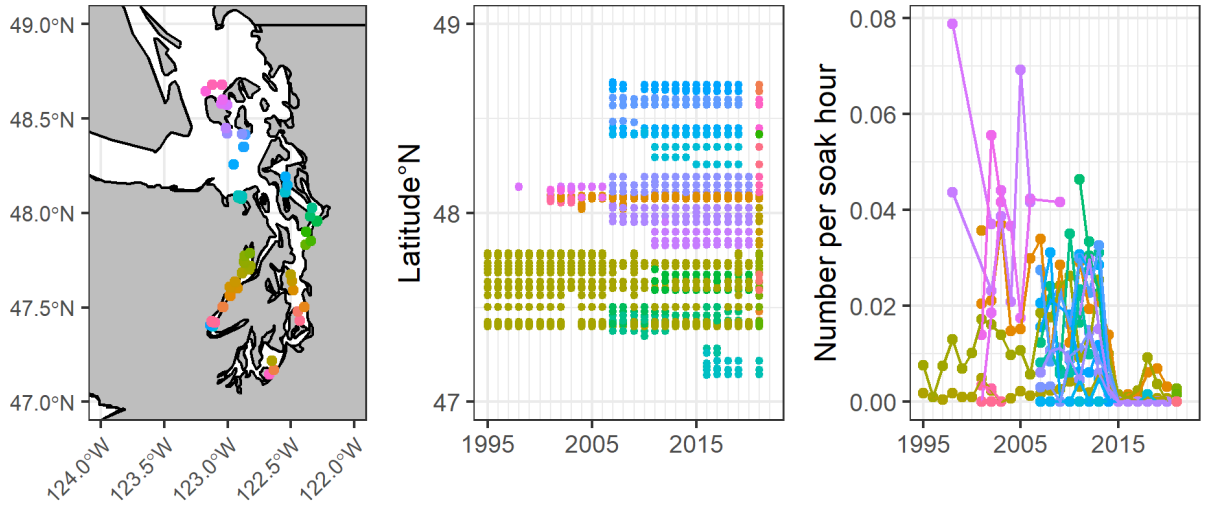


**Figure A3.28.** Location, data availability, and time series of *P. helianthoides* abundance in the WDFW shrimp test-fishery.

## A3.25 WDFW crab test-fishery (WDFW_crab)

In the WDFW crab test fishery (WDFW_crab), there are *P. helianthoides* observations running from 1999-2021 (Figure A3.29). The data are not density data but instead counts per soak time in hours. The test fishery operated in 371 locations, all of which were located in Hood Canal, Port Townsend Bay, or Kilisut Harbor. A time series of the mean *P. helianthoides* observed per hour of soak time was calculated by summing the total number of individuals observed in a location and dividing by the total number of hours soaked. For use in the MARSS analysis, these locations were averaged to produce one time series (Figure A3.29, right pane). These data were not used in the IUCN status assessment (Gravem et al. 2021) and show several peaks in abundance followed by rapid drop-offs, but the post-2013 reduction in encounters is most pronounced.

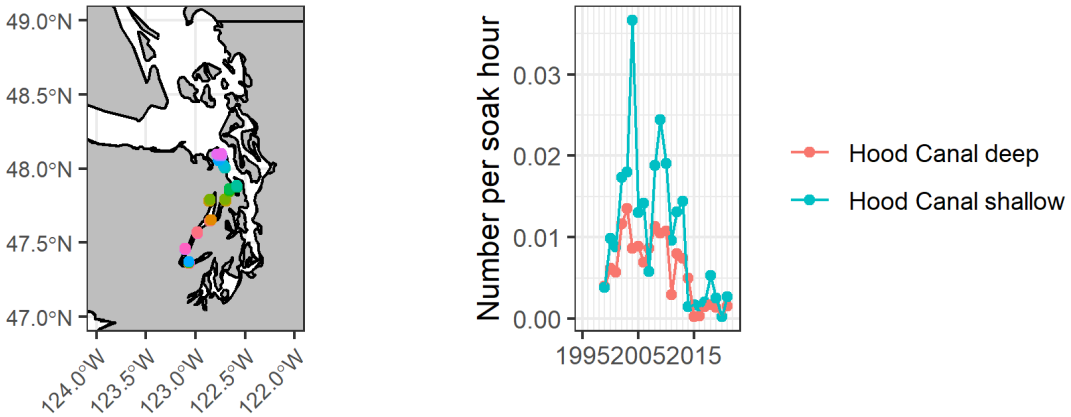


**Figure A3.29.** Location, and time series of *P. helianthoides* abundance in the WDFW crab test-fishery. Data for different locations have been summarized by depth bin for all of Hood Canal.

## A3.26 Watson Dive data, Vancouver Island (Watson_Dive_VanIs)

Watson dive data from Vancouver Island University (Watson_Dive_VanIs) for Vancouver Island, British Columbia, provide the longest data set, reaching back to 1987. They were summarized by site and year to calculate an annual average mean density (Figure A3.30). One location, Pacific Ocean, was actually two locations and relabeled as Pacific Ocean 1 and Pacific Ocean 2. The Watson dive sites are all located on the outer coast of Vancouver Island (Figure A3.30).

Interestingly, these data show a short-lived increase in *P. helianthoides* abundance after reaching essentially zero individuals in 2015, but abundance then decreased to zero at most locations. Ephemeral recruitment pules followed by a renewed die-off of individuals once they attain larger size/age (noted elsewhere) has been observed and may be the cause of this fluctuation in density.

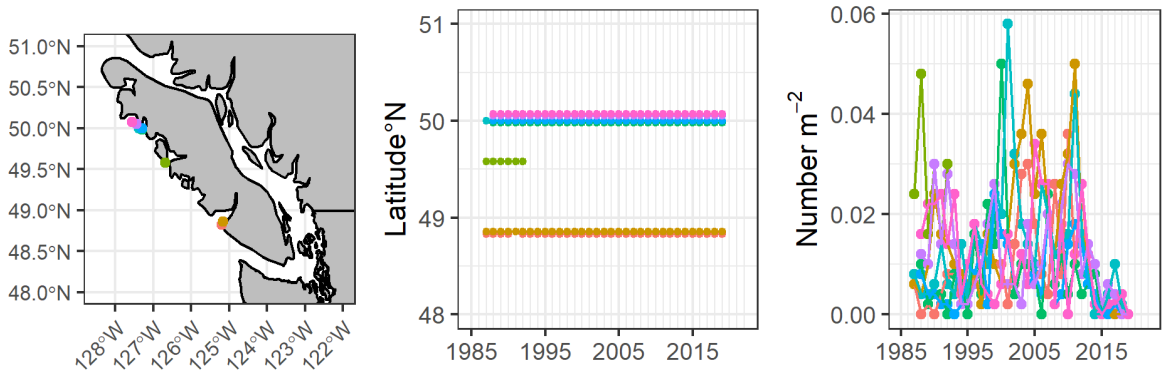


**Figure A3.30.** Location, availability, and time series of *P. helianthoides* density in the Watson dive surveys.

## A3.27 Williams et al. (2021) dive survey data (Williams_dive)

Williams et al. (2021) dive survey data (Williams_dive) cover 146 sites spread among 11 locations in southern California waters from 2011-21 (Figure A3.31). Data were summarized by location by calculating the mean density $m^{-2}$ of all sites within the location.

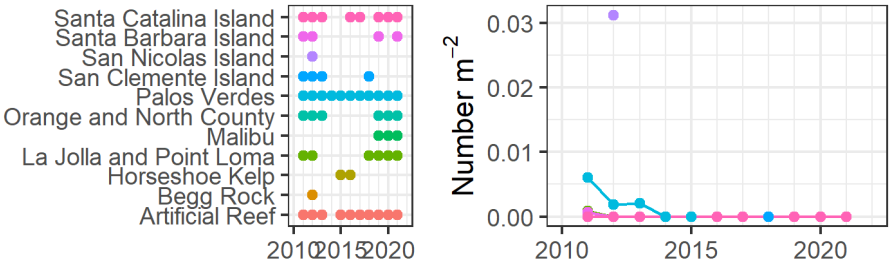


**Figure A3.31.** Data from the Williams et al. (2021) dive surveys. Note that in the right-hand pane, time series overlap, and no *P. helianthoides* were observed since 2013.

## A3.28 Time series used in the MARSS analyses

Table A3.4 shows the years covered by each data source used in the MARSS analysis. Figure A3.32 shows temporal availability of observations for each time series. Each row

represents an individual time series color coded by the data set. The colors repeat due to the large number of data sets, but are in the same order from top to bottom as the figure legend. After initial testing, some time series were removed because they were too short and, thus, uninformative (i.e., the model could not determine a trend with any confidence).

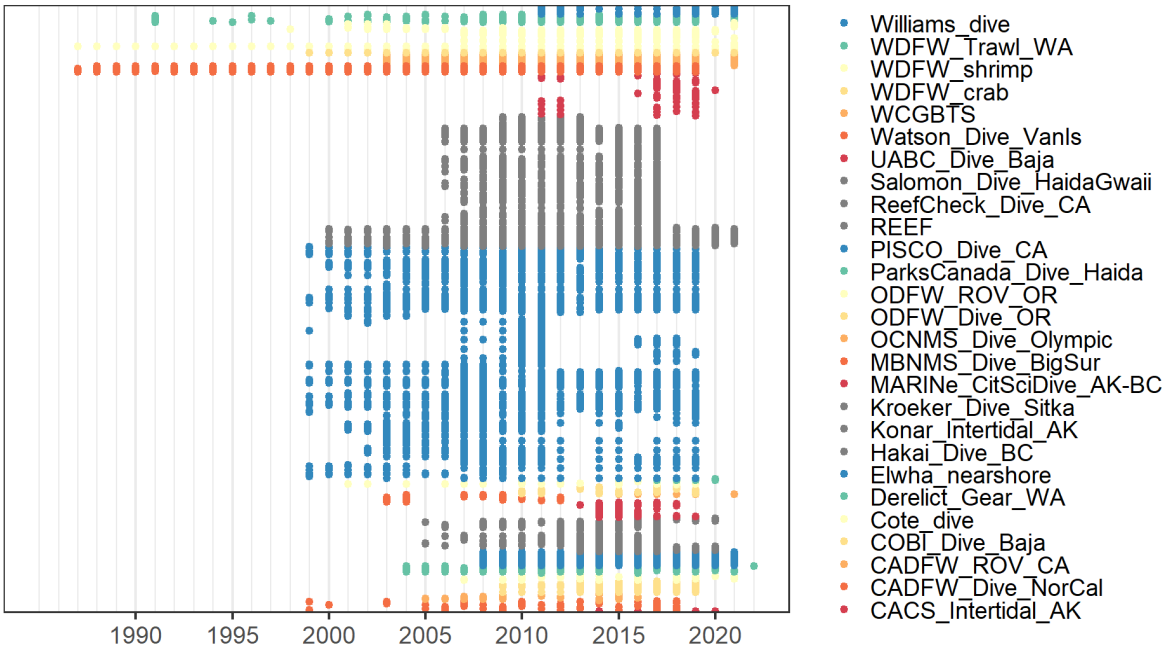


**Figure A3.32.** MARSS data availability by source and location. Points show years with density estimates. Note, the colors repeat but are ordered top to bottom on the figure and in the legend. The order is not based on latitude.

Tables A3.5-3.7 show the data available by region and data source when time series length was limited to five or more observations in an individual time series within data source and region. The tables show the available information under three different hypotheses about the spatial structure of *P. helianthoides* populations: three major regions, four major regions, and eleven regions. These regional structures were compared in the MARSS analysis that follows.

**Table A3.4.** Data sources used in the MARSS analyses including the years covered and data providers.

| Data source | Years | Institution | Contact | Email | New/Updated |
|---|---|---|---|---|---|
| CACS_Intertidal_AK | 2014-2020 | Center for Alaskan Coastal Studies | Katie Gavenus | katieg@akcoastalstudies.org | |
| CADFW_Dive_NorCal | 1999-2018 | California Department of Fish and Wildlife | Laura Rogers-Bennett, Shelby Kawana | | |
| CADFW_ROV_CA | 2005-2016 | CDFW and MARE. | Dirk Rosen and Mike Prall, Andy Lauermann | Michael@Wildlife, Dirk@maregroup.org, andy@maregroup.org | |
| COBI_Dive_Baja | 2009-2019 | Comunidad y Biodiversidad | Eduardo Diaz | ediaz@cobi.org.mx | |
| Cote_dive | 2007-2021 | Simon Fraser University | Isabelle Cote | imcote@sfu.ca | new |
| Derelict_Gear_WA | 2004-2022 | Washington State Derelict Fishing Gear Database, managed by the Northwest Straits Foundation | | | new |
| Elwha_nearshore | 2008-2021 | U.S. Geological Survey | Steve Rubin | srubin@usgs.gov | new |
| Hakai_Dive_BC | 2013-2020 | Hakai Institute | Alyssa Gehman | gehman@zoology.ubc.ca | |
| Konar_Intertidal_AK | 2005-2017 | Combination of USGS, National Park, Gulf Watch, UAF | Brenda Konar | bhkonar@alaska.edu | |
| Kroeker_Dive_Sitka | 2016-2020 | University of California Santa Cruz | Kristy Kroeker | kkroeker@ucsc.edu | |
| MARINe_CitSciDive_AK-BC | 2013-2019 | UCSC/MARINe/PISCO | Melissa Miner | cmminer@ucsc.edu | |
| MBNMS_Dive_BigSur | 2003-2012 | Monterey Bay National Marine Sanctuary | Steve Lonhart | steve.lonhart@noaa.gov | |
| OCNMS_Dive_Olympic | 2015-2021 | Olympic Coast National Marine Sanctuary/NOAA National Marine Fisheries Science | Jameal Samhouri, Ole Shelton, Greg Williams | ole.shelton@noaa.gov | updated |
| ODFW_Dive_OR | 2010-2019 | Oregon Department of Fish and Wildlife | Lindsay Aylesworth, Cori Kane | lindsay.x.aylesworth@state.or.us | |
| ODFW_ROV_OR | 2001-2019 | Oregon Department of Fish and Wildlife | Scott Marion | Scott.R.Marion@state.or.us | |
| ParksCanada_Dive_Haida | 2017-2020 | Parks Canada & Simon Fraser | Dan Okamoto, Lynn Lee | lynn.lee2@canada.ca, dokamoto@bio.fsu.edu | |
| PISCO_Dive_CA | 1999-2019 | Partnership for Interdisciplinary Studies of Coastal Oceans, University of California Santa Cruz, University of California Santa Barbara | Dan Malone | dmalone@ucsc.edu | |
| REEF | 2000-2021 | Reef Environmental Education Foundation | Christy Semmens | christy@reef.org | new |
| ReefCheck_Dive_CA | 2006-2017 | Reef Check | Jan Friewald | freiwald@ucsc.edu | |
| Salomon_Dive_HaidaGwaii | 2009-2013 | Simon Fraser University | Anne Solomon | anne_salomon@sfu.ca | |
| UABC_Dive_Baja | 2011-2020 | Universidad Autonoma de Baja California | Rodrigo Baes-Luna, Guillermo Torres-Moye | rbeas@uabc.edu.mx, gtorres@uabc.edu.mx | |
| Watson_Dive_VanIs | 1987-2019 | | | | |
| WCGBTS | 2003-2021 | NOAA- National Marine Fisheries Science | Aimee Keller | aimee.keller@noaa.gov | updated |
| WDFW_crab | 1999-2021 | Washington Department of Fish and Wildlife | | | new |
| WDFW_shrimp | 1987-2021 | Washington Department of Fish and Wildlife | Shellfish Management Team, Daniel Sund | Daniel.Sund@dfw.wa.gov | new |
| WDFW_Trawl_WA | 1991-2021 | Washington Department of Fish and Wildlife | Marine Fish Science Unit, Jennifer Blaine | Jennifer.Blaine@dfw.wa.gov | |
| Williams_dive | 2011-2021 | Occidental College | Jon Williams | jonwilliams@oxy.edu | new |

**Table A3.5.** Number of time series used in the MARSS analysis by three major regions and data source. N is the total number of time series within a larger region. n is the number of time series by data source.

| Region | N | Data source | n |
|---|---|---|---|
| Alaska | 24 | CACS_Intertidal_AK | 2 |
| | | Konar_Intertidal_AK | 20 |
| | | Kroeker_Dive_Sitka | 2 |
| BC and Salish Sea | 90 | Cote_dive | 3 |
| | | Elwha_nearshore | 16 |
| | | Hakai_Dive_BC | 7 |
| | | MARINe_CitSciDive_AK-BC | 3 |
| | | REEF | 12 |
| | | Salomon_Dive_HaidaGwaii | 6 |
| | | Watson_Dive_VanIs | 8 |
| | | WDFW_crab | 2 |
| | | WDFW_shrimp | 17 |
| | | WDFW_Trawl_WA | 16 |
| West Coast | 278 | CADFW_Dive_NorCal | 8 |
| | | CADFW_ROV_CA | 2 |
| | | COBI_Dive_Baja | 14 |
| | | MBNMS_Dive_BigSur | 4 |
| | | OCNMS_Dive_Olympic | 1 |
| | | ODFW_Dive_OR | 3 |
| | | ODFW_ROV_OR | 2 |
| | | PISCO_Dive_CA | 147 |
| | | REEF | 9 |
| | | ReefCheck_Dive_CA | 68 |
| | | WCGBTS | 15 |
| | | Williams_dive | 5 |

**Table A3.6.** Number of time series used in the MARSS analysis by four major regions and data source. N is the total number of time series within a larger region. n is the number of time series by data source.

| Region | N | Data source | n |
|---|---|---|---|
| Alaska | 24 | CACS_Intertidal_AK | 2 |
| | | Konar_Intertidal_AK | 20 |
| | | Kroeker_Dive_Sitka | 2 |
| British Columbia | 25 | Cote_dive | 2 |
| | | Hakai_Dive_BC | 7 |
| | | REEF | 2 |
| | | Salomon_Dive_HaidaGwaii | 6 |
| | | Watson_Dive_VanIs | 8 |
| Salish Sea | 65 | Cote_dive | 1 |
| | | Elwha_nearshore | 16 |
| | | MARINe_CitSciDive_AK-BC | 3 |
| | | REEF | 10 |
| | | WDFW_crab | 2 |
| | | WDFW_shrimp | 17 |
| | | WDFW_Trawl_WA | 16 |
| West Coast | 278 | CADFW_Dive_NorCal | 8 |
| | | CADFW_ROV_CA | 2 |
| | | COBI_Dive_Baja | 14 |
| | | MBNMS_Dive_BigSur | 4 |
| | | OCNMS_Dive_Olympic | 1 |
| | | ODFW_Dive_OR | 3 |
| | | ODFW_ROV_OR | 2 |
| | | PISCO_Dive_CA | 147 |
| | | REEF | 9 |
| | | ReefCheck_Dive_CA | 68 |
| | | WCGBTS | 15 |
| | | Williams_dive | 5 |

**Table A3.7.** Number of time series used in the MARSS analysis by eleven regions and data source. N is the total number of time series within a larger region. n is the number of time series by data source.

| Region | N | Data source | n |
|---|---|---|---|
| Baja California | 14 | COBI_Dive_Baja | 14 |
| British Columbia | 25 | Cote_dive | 2 |
| | | Hakai_Dive_BC | 7 |
| | | REEF | 2 |
| | | Salomon_Dive_HaidaGwaii | 6 |
| | | Watson_Dive_VanIs | 8 |
| Central California | 98 | MBNMS_Dive_BigSur | 4 |
| | | PISCO_Dive_CA | 73 |
| | | ReefCheck_Dive_CA | 18 |
| | | WCGBTS | 3 |
| East Gulf of Alaska | 17 | CACS_Intertidal_AK | 2 |
| | | Konar_Intertidal_AK | 15 |
| Northern California | 29 | CADFW_Dive_NorCal | 8 |
| | | PISCO_Dive_CA | 10 |
| | | ReefCheck_Dive_CA | 8 |
| | | WCGBTS | 3 |
| Oregon | 14 | ODFW_Dive_OR | 3 |
| | | ODFW_ROV_OR | 2 |
| | | PISCO_Dive_CA | 2 |
| | | REEF | 4 |
| | | WCGBTS | 3 |
| Salish Sea | 65 | Cote_dive | 1 |
| | | Elwha_nearshore | 16 |
| | | MARINe_CitSciDive_AK-BC | 3 |
| | | REEF | 10 |
| | | WDFW_crab | 2 |
| | | WDFW_shrimp | 17 |
| | | WDFW_Trawl_WA | 16 |
| Southeast Alaska | 2 | Kroeker_Dive_Sitka | 2 |
| Southern California | 118 | CADFW_ROV_CA | 2 |
| | | PISCO_Dive_CA | 62 |
| | | REEF | 4 |
| | | ReefCheck_Dive_CA | 42 |
| | | WCGBTS | 3 |
| | | Williams_dive | 5 |
| Washington | 5 | OCNMS_Dive_Olympic | 1 |
| | | REEF | 1 |
| | | WCGBTS | 3 |
| West Gulf of Alaska | | Konar_Intertidal_AK | 5 |

## A4 Multivariate Autoregressive State Space (MARSS) Modeling

Multivariate autoregressive state space models (MARSS) were used to estimate *P. helianthoides* population trends (Holmes et al. 2012; Tolimieri et al. 2017; Holmes et al. 2021). More specifically, MARSS was used to estimate a time-varying rate of population growth/decline with pre- and post-2013 estimates of population rates of change. This approach provides an understanding of trends in *P. helianthoides* abundance prior to the onset of SSWS in 2013, then also models the observed population decline during the epidemic collapse. MARSS was also used to estimate process variance, which is important for evaluating extinction risk. In addition, comparison of multiple models and model selection criteria was used to investigate hypotheses related to the spatial structure of *P. helianthoides* population processes and the combining of data sources.

Data sets used here came from multiple data sources with different methodologies, are of different time-series length, and many are "gappy" with missing observations in individual years (see section A3 Data Sources). MARSS allows one to overcome these multiple hurdles often associated with population viability analyses (PVA) using time series data (Tolimieri et al. 2017; Holmes et al. 2021) because MARSS can:

- combine time series from different data sources or methodologies (e.g., dive surveys and trawl surveys) through the inclusion of a scaling parameter.
- allow different time series to estimate a common population growth rate while having different process variance and/or error variance.
- handle "gappy" or fragmented time series with missing data (i.e., missing observations in a year) and of different length through the use of a Kalman filter (Holmes et al. 2021), which also allows the merger of time series of differing lengths.
- implement spatial replication, which helps to separate process and observational variance. Given the generally short nature of the time series here, this spatial replication is important. For *P. helianthoides* spatial replication comes from both time series in different regions and also multiple different data sources.

Models employed in MARSS analyses consist of two equations. The $x$ equation estimates the state process, in this case the predicted population trends for *P. helianthoides* (trend and state, or state process, are used interchangeably in the following text). The observed data $y_t$ then enter the $y$ equation, which estimates the observation process and contains the model structure. The two equations are:

$$x_t = B_t x_{t-1} + u_t \; where \; w_t \sim MVN(0, Q_t)$$

$$y_t = Z_t x_t + a_t \; where \; v_t \sim MVN(0, R_t)$$

In the $x$ equation, the realized state (population trend or trajectory) $x$ at year $t$ is dependent upon the previous year's state $x_{t-1}$ plus the population growth rate $u_t$, which is the rate of population decline if $u$ is negative. For example, population size in 2020 is a

function of population size in 2019 plus the population growth rate. It is the $u$ parameter that is primarily of interest for the PVA. The $B$ term is a species interaction matrix and accounts for density-dependence in both intra- and in some models inter-specific interactions. Here this term was set to $B_t = 1$ (an identity matrix), or an assumption of density-independence, because it is not possible to estimate both $u$ and $B$ and because *P. helianthoides* were either declining or that are well below historical levels (Holmes et al. 2021). The term $w_t$ is a matrix of processes errors at time $t$; these are multivariate normal with $Q$ is the process variance-covariance matrix. Process variance represents real, biological variation in the trend over time, variation due to some un-observed variable, such as inter-annual variation in recruitment or survival.

Observed data enter the $y$ equation where $Z$ is a design matrix and $a$ is a scaling parameter. The $Z$ term defines the number of states, or realized time series. Comparing different $Z$ structures and allows one to evaluate hypotheses related to space (combining or separating regions, for example) and to evaluate combining or separating different data sources. The scaling parameter $a$ accounts for different scales among data sources and functions somewhat like an estimate of catchability (Tolimieri et al. 2017). The term $v_t$ is a matrix of observation errors at time $t$; these are multivariate normal, and $R$ is the observation variance-covariance matrix.

Here, the analysis is primarily interested in estimating the population growth rate $u$ and the process variance $Q$, which feed into extinction risk calculations. The structure of $Z$ and $u$ provide information about the spatial structure of the population and population processes. For example, there can be one population trend or trajectory in $Z$ for the entire northeastern Pacific Ocean or multiple trends for each region, as defined below. Additionally, there can be one rate of population growth for all regions or the rate can vary among regions.

It is common to log-transform data for MARSS analysis to stabilize variance, so original data were scaled as:

$$N_t = N_{t-1} * exp(u)$$

where $N_t$ and $N_{t-1}$ are population size in year $t$ and in the preceding year, and $100 * (exp(u) - 1)$ is the percent change in population size per year. All analyses were conducted in R version 4.2.0 (Harvey et al. 2022) using the 'MARSS' package (Holmes et al. 2021). See Tolimieri et al. (2017) and Holmes et al. (2021) for more detail.

## A4.1 Model fitting

Prior to analysis, time-series data were log-transformed as described above. The exception was the REEF data, which were already on a pseudo-log scale and were left untransformed. Observations of zero (0) *P. helianthoides* were converted to 'NA'. A zero assumes that there were absolutely no individuals present, which may not be true. Abundance may have been low enough to make observation of *P. helianthoides* unlikely, but they may have still been above zero density. The NA allows MARSS, through the use of Kalman filters, to approximate abundance based on the population trend and estimated model parameters (Tolimieri et al. 2017; Holmes et al. 2021). However, additional models were fit to test the

sensitivity of the best-fit and other models to replacing zeros with NA values. For these additional models, zero observations were replaced with a minimum value derived separately for each data source (discussed more fully below). Models were fit with the Broyden–Fletcher–Goldfarb–Shanno (BFGS) algorithm because process errors were small or near zero for some time series. Time series with fewer than five years of data were excluded from the analysis.

## A4.2 Model comparison

Model selection was used to evaluate data support for multiple model structures representing different hypotheses about the spatial structure of *P. helianthoides* population trends ($Z$, states) and population growth rates ($u$). In addition, data support for combining data sources within regions ($Z$, states) and different process error structure ($Q$) were also investigated. Model selection was based on Akiake's Information Criterion for small sample sizes (AICc) (Burnham and Anderson 1998) and the total number of parameters. Models with $\Delta$AICc $\leq$ 2.0 were considered candidate models, and the model with the fewest parameters and a $\Delta$AICc $\leq$ 2.0 was considered the best-fit model.

## A4.3 Model structures

Data support for the following model structures was evaluated:

**Z-matrix - One overall state process or multiple processes by region:** The design matrix $Z$ was coded to evaluate different regional structures with either one overall state process for the entire range or different state process for different regional agglomerations:

- One state process for the entire Northeast Pacific from Alaska to Baja California
- Three major regions: Alaska, British Columbia & the Salish Sea, and the West Coast
- Four major regions: Alaska, British Columbia, the Salish Sea, and the West Coast
- Eleven regions similar to those used in Hamilton et al. (2021) and the IUCN Red List report (Gravem et al. 2021), but excluding the Aleutian Islands due to lack of data: west Gulf of Alaska, east Gulf of Alaska, southeast Alaska, British Columbia, Salish Sea, Washington, Oregon, Northern California, Central California, Southern California, and Baja California.

**Z-matrix - Separate state process by data source or combined within region:** Additionally, the design matrix $Z$ was coded to evaluate data support for combining or separating data sources. The $Z$ structures above assume that data can be combined by data source within regions. Here, the data sources are treated as different state process or trends for each level of regional aggregation above:

- Three regions x source
- Four regions x source
- Eleven regions x source

**u - Equal or unique population growth rate across states:** Because *P. helianthoides* populations began to crash with the onset of SSWS in approximately 2013, though this varied by region, all models included time-varying population growth rate $u$ and estimated

pre-2013 and post-2013 $u_t$. In addition, the following $u$ structures within each time periods were evaluated:

- A common $u$ for all regions. These models produce only two $u$ estimates: one for the early period and one for 2013-21, and hypothesize that all regions declined at the same rate.
- Different $u$ for each region. These models produce one $u$ for each region before and after 2013. This option did not include separate $u$ by region x source estimate, in part due to the large computation costs and extended computing time to estimate these such models, and in part because the focus was on detecting regional variability. This approach essentially averages $u$ within regions across data sources.

**Q-matrix - Equal or unique process variance (Q-matrix) across states:** Two structures were evaluated for the variance-covariance matrix $Q$:

- Diagonal and equal: all states have the same process variance, no covariance
- Diagonal and unequal: states have different process variance, no covariance

More complex models with covariance (i.e., values on the off diagonal of $Q$) were investigated, but proved too time consuming to fit due to the large number of parameters and, in some areas, relatively sparse data.

**R-matrix:** The R matrix gives the structure of the observation error. Only one $R$ structure was evaluated because estimating different observation error by data source proved prohibitive in terms of processing time:

- Diagonal and equal - all states had the same observation error

The minimum time series length was set to five. This reduced the data matrix from 752 individual time series to 392. Nevertheless, substantial data were missing, making the overall data-to-parameter ratio low and likely resulting in a fairly flat likelihood, which required long run-times to fit each model (>24 hrs in some cases).

## A4.4 Model sensitivity to replacing zeros with NAs.

Many of the time series contain a large number of zero observations, especially in the later part of the time series after the onset of SSWS. In the primary model comparisons, these zero values were set to 'NA', which is not uncommon for MARSS-style analyses. Retaining the zero (0) observation asserts that there were no *P. helianthoides* present, though presence at a very low density beyond detection given survey method and effort is more likely. Setting the zeros to NA allows the model to estimate those values through the use of a Kalman filter. However, using the NAs may underestimate the rate of decline, especially in cases where there are large numbers of zeros in the latter portion of the time series.

Replacing zeros with some other small value was also investigated for the best-fit model (hereafter, best-fit w/NA or best-fit w/min) and region-specific models, which included only data for one of the three major regions. Initial runs were investigated setting the zero-replacement value to a proportion of the minimum, non-zero, observed value for each data source or methodology (e.g., dive vs trawl) (Table A4.1). However, this approach produced

a wide-range of ratios between replacement values among the time series. In some cases, the approach limited the zero-replacement value to a relatively high proportion of the mean of the observed time series, which would bias the results to lower rates of population decline, and initial models runs using this approach produced unreasonably small rates of population decline for the post-2013 period. Instead, the zero-replacement value was set to $y_{replacement} = mean(y_{datasource})$*0.001 (Table A4.1), so that all time series could estimate the same proportional decline relative to the mean of that time series.

## A4.5 Comparing model results

To better compare model results, two metrics were calculated from the model output:

- Annual percent growth rate = $100 * (exp(u) - 1)$
- Percent decline since 2013 = $100 - 100 * exp(u)^{(2022-2013)}$

The calculations assume that $N_t = N_{t-1} * r$ and that $N_t = N_i * r^{t-i}$, $N_t$ is the current population size ($N_{2022}$), $N_i$ is population size in 2013 ($N_{2013}$), and $r = exp(u)$. For percent decline since 2013, $N_{2013}$ was set to 100 to express the current size as a percentage of $N_{2013}$.

## A4.6 MARSS Results

### A4.6.1 Best-fit model

There was one model with $\Delta AICc \leq 2.0$ (Table A4.2), and this was chosen as the best-fit model (below this is "best-fit w/NA"). It had an AICc value 8.39 points lower than the second best model and 424 estimated parameters.

The best-fit model (Model 1, Table A4.3) had a three regions x source $Z$ structure and 25 state processes (data sources within the three regions). This model included separate process variance for each state. However, the model varied in its ability to estimate process variance, with some states having zero or extremely low process variance (Table A4.3) due to the shortness of some time series and lack of spatial replication.

The second best model (Table A4.2) provided some weak data support for splitting British Columbia and the Salish Sea. It had a four regions x source states-structure ($Z$), and separate population growth rates by region.

The best-fit model estimated separate rates of population growth for each of the three regions within each time period (pre and post 2013, Table A4.3, Figures A4.1-4.3).

For the West Coast and combined British Columbia and Salish Sea region, *P. helianthoides* abundance increased during the period prior to the onset of SSWS (pre-2013) at 1.7% ($u$=0.017) and 9.4% ($u$=0.09), respectively (Table A4.3). Post 2013, West Coast populations declined rapidly at 25.8% ($u$ =-0.299) annually. The rate of decline in British Columbia and the Salish Sea was somewhat less, but still substantial at 14.1% ($u$ =-0.151) annually.

**Table A4.1.** Minimum non-zero values observed in the data sets by methodology and data type. In some models, zeros were replaced with the Zero replacement value to test the sensitivity of models to replacing zeros with NAs. The Zero replacement value is the minimum non-zero for that methodology and data type multiplied by 0.25.

| Data source | Maximum | Mean | Minimum | Ratio | Method | Data type | Zero replacement |
|---|---|---|---|---|---|---|---|
| CACS_Intertidal_AK | 0.21000 | 0.056324 | 0.000408 | 138:1 | intertidal | density m2 | 0.000056324 |
| CADFW_Dive_NorCal | 0.08542 | 0.029029 | 0.000463 | 63:1 | dive survey | density m2 | 0.000029029 |
| CADFW_ROV_CA | 0.01559 | 0.006942 | 0.000020 | 347:1 | ROV | density m2 | 0.000006942 |
| COBI_Dive_Baja | 0.02500 | 0.007508 | 0.000617 | 12:1 | dive survey | density m2 | 0.000007508 |
| Cote_dive | 28.00000 | 12.283939 | 1.313333 | 9:1 | dive survey | mean counts | 0.012283939 |
| Elwha_nearshore | 0.17500 | 0.042998 | 0.016667 | 3:1 | dive survey | density m2 | 0.000042998 |
| Hakai_Dive_BC | 0.08333 | 0.015611 | 0.000633 | 25:1 | dive survey | density m2 | 0.000015611 |
| Konar_Intertidal_AK | 0.86000 | 0.068807 | 0.002500 | 28:1 | intertidal | density m2 | 0.000068807 |
| Kroeker_Dive_Sitka | 0.02917 | 0.012004 | 0.002083 | 6:1 | dive survey | density m2 | 0.000012004 |
| MARINe_CitSciDive_AK-BC | 0.10833 | 0.033635 | 0.008333 | 4:1 | dive survey | density m2 | 0.000033635 |
| MBNMS_Dive_BigSur | 0.01102 | 0.004124 | 0.001471 | 3:1 | dive survey | density m2 | 0.000004124 |
| OCNMS_Dive_Olympic | 0.00156 | 0.000873 | 0.000270 | 3:1 | dive survey | density m2 | 0.000000873 |
| ODFW_Dive_OR | 0.06333 | 0.028731 | 0.001852 | 16:1 | dive survey | density m2 | 0.000028731 |
| ODFW_ROV_OR | 0.05450 | 0.023719 | 0.000159 | 149:1 | ROV | index | 0.000023719 |
| PISCO_Dive_CA | 1.02500 | 0.065138 | 0.004167 | 16:1 | dive survey | density m2 | 0.000065138 |
| REEF | 3.00000 | 1.528571 | 0.010309 | 148:1 | dive survey | index | 0.001528571 |
| ReefCheck_Dive_CA | 0.15833 | 0.021343 | 0.001389 | 15:1 | dive survey | density m2 | 0.000021343 |
| Salomon_Dive_HaidaGwaii | 0.12500 | 0.047178 | 0.008333 | 6:1 | dive survey | density m2 | 0.000047178 |
| Watson_Dive_VanIs | 0.05800 | 0.013280 | 0.002000 | 7:1 | dive survey | density m2 | 0.000013280 |
| WCGBTS | 0.00030 | 0.000048 | 0.000002 | 24:1 | trawl | kg m-2 | 0.000000048 |
| WDFW_crab | 0.03659 | 0.008298 | 0.000252 | 33:1 | soak time | soak time | 0.000008298 |
| WDFW_shrimp | 0.06915 | 0.013823 | 0.000386 | 36:1 | soak time | soak time | 0.000013823 |
| WDFW_Trawl_WA | 0.00767 | 0.000387 | 0.000004 | 97:1 | trawl | density m2 | 0.000000387 |
| Williams_dive | 0.00609 | 0.002700 | 0.000833 | 3:1 | dive survey | density m2 | 0.000002700 |

The results for Alaska from this best-fit model should be interpreted cautiously, at least for the pre-2013 period. The model estimated a decline in *P. helianthoides* abundance in the pre-SSWS period of 19% annually ($u$ =-0.21) and an incredibly steep decline in the post-SSWS period from 2013-21 of 91.6% annually ($u$ =-2.475). However, there are very few time-series data in the pre-2013 period, with the Konar_Intertidal_AK data set being the only source of pre-2013 information. Furthermore, this data series extends back to only 2005 (Table A3.4), falling well short of the temporal coverage available in other regions. Observation error balloons in the pre-2013 period for the CACS_Intertidal_AK data set (Figure A4.3), and the process variance for the CACS_Intertidal_AK data set is very large (Table A4.3), suggesting that the model is struggling to fit this time series. Moreover, it is this time series state that is driving the negative $u$ during the pre-2013 period, without any data supporting that negative trend (Figure A4.3). Estimates for this period in Alaska in the best-fit model are likely being driven by low data availability, low $Q$, and low $R$ resulting from data sharing from the rest of available data.

**Table A4.2.** Results of the MARSS analysis model fitting showing delta AIC and AICC values for the candidate models. Z = state processes, U = population growth rate, Q = process variance-covariance matrix, R = observation variance-covariance matrix, AICc = Akiake's Information Criterion, D_AICc = delta AICc, Params = number of estimated parameters. Note, the structure of Q and R is based on Z, while U differs as shown. de = diagonal and equal, du = diagonal and unequal. All models included a time-varying U with pre-2013 and post-2013 estimates of population growth rate.

| Model | Z | U | Q | R | AICc | D_AICc | Params |
|---|---|---|---|---|---|---|---|
| Model 1 | Three regions x source | Three regions | du | de | 6,559.8 | 0.0 | 424 |
| Model 2 | Four regions x source | Four regions | du | de | 6,568.2 | 8.4 | 428 |
| Model 3 | source | Equal | du | de | 6,568.9 | 9.1 | 419 |
| Model 4 | Three regions x source | Equal | du | de | 6,572.4 | 12.6 | 420 |
| Model 5 | region | Equal | Q | de | 6,580.6 | 20.8 | 434 |
| Model 6 | Four regions x source | Equal | du | de | 6,581.6 | 21.8 | 422 |
| Model 7 | Source | Source | du | de | 6,605.8 | 46.0 | 465 |
| Model 8 | Source | Equal | de | de | 6,621.2 | 61.4 | 396 |
| Model 9 | 11 regions | Equal | du | de | 6,623.6 | 63.8 | 406 |
| Model 10 | Three regions x source | Three regions | de | de | 6,632.9 | 73.1 | 400 |
| Model 11 | Three regions x source | Equal | de | de | 6,633.9 | 74.1 | 396 |
| Model 12 | 11 regions | Equal | de | de | 6,634.0 | 74.2 | 396 |
| Model 13 | Four regions x source | Equal | de | de | 6,645.9 | 86.1 | 396 |
| Model 14 | Four regions x source | Four regions | de | de | 6,648.4 | 88.6 | 402 |
| Model 15 | region | Source | Q | de | 6,648.5 | 88.7 | 504 |
| Model 16 | 11 regions x source | Equal | de | de | 6,653.8 | 94.0 | 396 |
| Model 17 | Four regions | Equal | du | de | 6,656.2 | 96.4 | 399 |
| Model 18 | Four regions | Equal | de | de | 6,660.7 | 100.9 | 396 |
| Model 19 | 11 regions | 11 regions | de | de | 6,663.0 | 103.2 | 416 |
| Model 20 | Four regions | Four regions | du | de | 6,665.7 | 105.9 | 405 |
| Model 21 | Source | Source | de | de | 6,666.3 | 106.5 | 442 |
| Model 22 | Four regions | Four regions | de | de | 6,670.3 | 110.5 | 402 |
| Model 23 | Three regions | Equal | de | de | 6,677.4 | 117.6 | 396 |
| Model 24 | Three regions | Equal | du | de | 6,677.8 | 118.0 | 398 |
| Model 25 | Three regions | Three regions | de | de | 6,683.0 | 123.2 | 400 |
| Model 26 | Three regions | Three regions | du | de | 6,684.8 | 125.0 | 402 |
| Model 27 | 11 regions | 11 regions | du | de | 6,699.8 | 140.0 | 426 |
| Model 28 | 11 regions x source | 11 regions | de | de | 6,736.4 | 176.6 | 472 |

Three regions: Alaska, British Columbia & the Salish Sea, and West Coast.

Four regions: Alaska, British Columbia, Salish Sea, and West Coast

Eleven regions: west Gulf of Alaska, east Gulf of Alaska, southeast Alaska, British Columbia, Salish Sea, Washington, Oregon, Northern California, Central California, Southern California, and Baja California

**Table A4.3.** Selected model coefficients for the best-fit model. Best-fit w/NA is Model 1 from the main model comparison exercise. Best-fit w/min has the same model structure and is included as a test of model sensitivity to replacing zeros with NAs. In this second model, the zeros in the data set were replaced with minimum values determined as 0.001 times the mean of the data source. See below for more information on determining this zero-replacement value. U.t1 and Ut.1 are population growth rates pre-2013 and post-2013, respectively, for each region as defined by Z. Q = process variance, R.diag = observation variance. The scaling factor A has been omitted.

| Parameter | Best-fit w/NA | Best-fit w/min |
|---|---|---|
| U.t1-Alaska | -0.210 | -0.069 |
| U.t1-BC and Salish Sea | 0.090 | 0.129 |
| U.t1-West Coast | 0.017 | -0.021 |
| U.t2-Alaska | -2.475 | -1.447 |
| U.t2-BC and Salish Sea | -0.151 | -0.384 |
| U.t2-West Coast | -0.299 | -0.246 |
| Q.Alaska_CACS_Intertidal_AK | 10.295 | 1.970 |
| Q.West Coast_CADFW_Dive_NorCal | 0.339 | 0.000 |
| Q.West Coast_CADFW_ROV_CA | 0.000 | 0.483 |
| Q.West Coast_COBI_Dive_Baja | 0.000 | 0.000 |
| Q.BC and Salish Sea_Cote_dive | 0.059 | 0.767 |
| Q.BC and Salish Sea_Elwha_nearshore | 0.000 | 2.663 |
| Q.BC and Salish Sea_Hakai_Dive_BC | 0.399 | 1.738 |
| Q.Alaska_Konar_Intertidal_AK | 0.226 | 0.791 |
| Q.Alaska_Kroeker_Dive_Sitka | 0.000 | 2.739 |
| Q.BC and Salish Sea_MARINe_CitSciDive_AK-BC | 0.000 | 0.000 |
| Q.West Coast_MBNMS_Dive_BigSur | 0.000 | 0.000 |
| Q.West Coast_WCGBTS | 0.456 | 1.290 |
| Q.West Coast_OCNMS_Dive_Olympic | 0.000 | 14.957 |
| Q.West Coast_ODFW_Dive_OR | 0.111 | 4.961 |
| Q.West Coast_ODFW_ROV_OR | 1.122 | 1.697 |
| Q.West Coast_PISCO_Dive_CA | 0.059 | 0.832 |
| Q.West Coast_ReefCheck_Dive_CA | 0.126 | 0.778 |
| Q.BC and Salish Sea_REEF | 0.045 | 0.000 |
| Q.West Coast_REEF | 0.000 | 0.000 |
| Q.BC and Salish Sea_Salomon_Dive_HaidaGwaii | 0.000 | 0.000 |
| Q.BC and Salish Sea_WDFW_Trawl_WA | 0.283 | 0.551 |
| Q.BC and Salish Sea_WDFW_shrimp | 0.057 | 0.695 |
| Q.BC and Salish Sea_WDFW_crab | 0.225 | 0.000 |
| Q.BC and Salish Sea_Watson_Dive_VanIs | 0.016 | 0.539 |
| Q.West Coast_Williams_dive | 0.000 | 0.000 |
| R.diag | 0.431 | 2.816 |

### A4.6.2 Sensitivity to zeros

Running the same overall model structure as the best-fit w/NA model but replacing the zeros with minimum values (best-fit w/min) produced some relatively minor differences in estimates of population growth (Table A4.3) for the West Coast. For example, the rate of population decline changed from $u_{postNA}$ = -0.299 to $u_{postMin}$ = -0.246 or from -26% per year to -22% per year. However, the rate of decline for the combined British Columbia and Salish Sea regions increased substantially from $u_{postNA}$ = -0.151 to $u_{postMin}$ = -0.384, or from -14% per year to -30% per year. Estimates for Alaska showed a slower rate of decline when zeros were replaced with minimum values with the parameter changing from $u_{postNA}$ = -2.475 to $u_{postMin}$ = -1.447, or from -92% per year to -76% per year.

Replacing NAs with minimum values lead to substantial increases in observational variance (Table A4.3, Figures A4.1-4.3). In the best-fit w/min model, the large estimate of process variance shifted to the OCNMS dive survey time series in the West Coast region, likely because of zeros earlier in the time series (Figure A3.17). In the best-fit w/NA model, these NAs would have been interpolated via the Kalman filter resulting in a smoother estimated state without large fluctuations. However, with the best-fit w/min model the resulting state is more variable, resulting in large process variance (Figure A4.1).

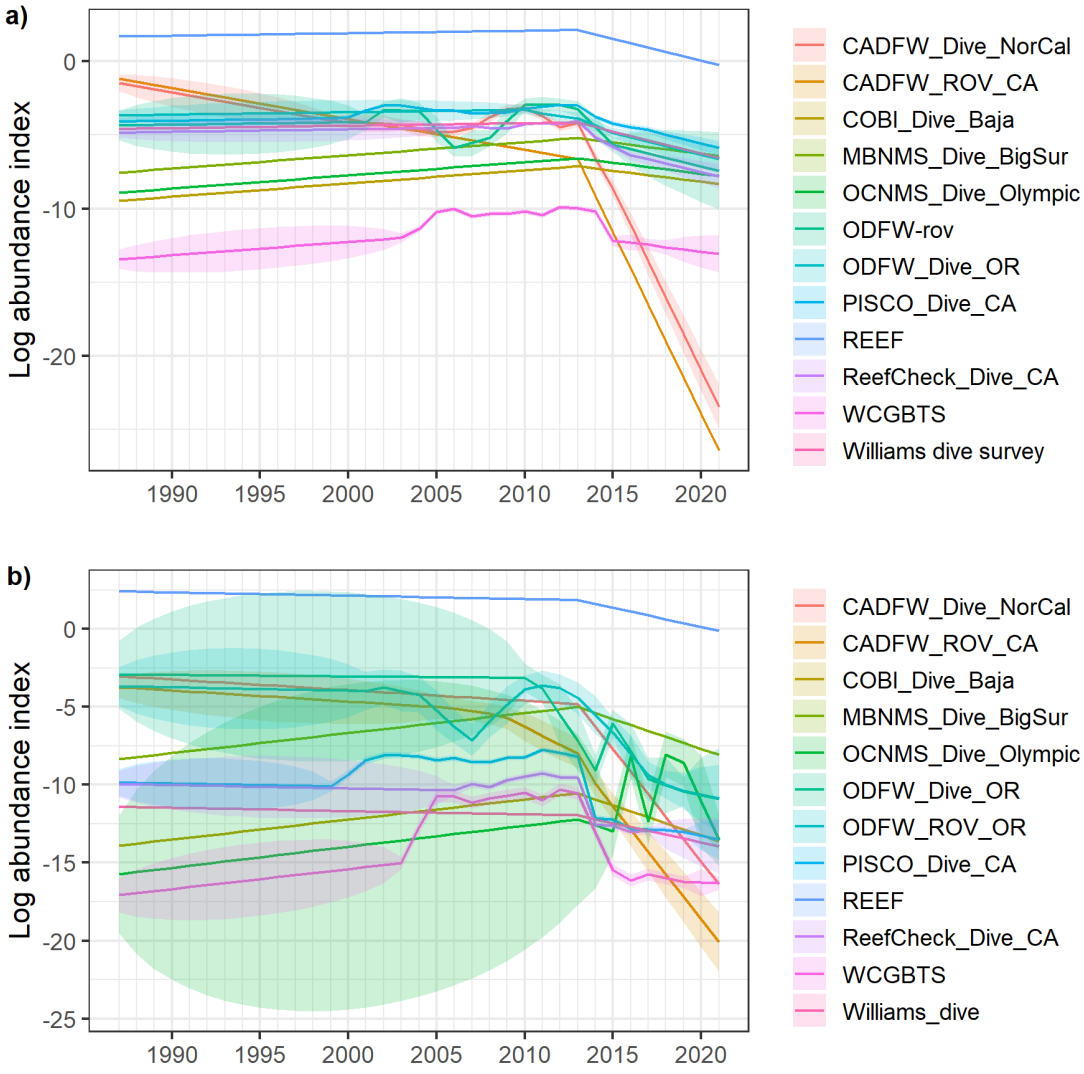


**Figure A4.1.** Log abundance index of *P. helianthoides* on the West Coast from 1987-2021 based on MARSS analysis. a) results from the best-fit model with zeros replaced by NAs; b) results from the model with zeros replaced by a minimum value. Error envelopes indicate one standard error. Note, the inflated errors in some time series (pre-1999) occur because there are no data for that time series in that time period.

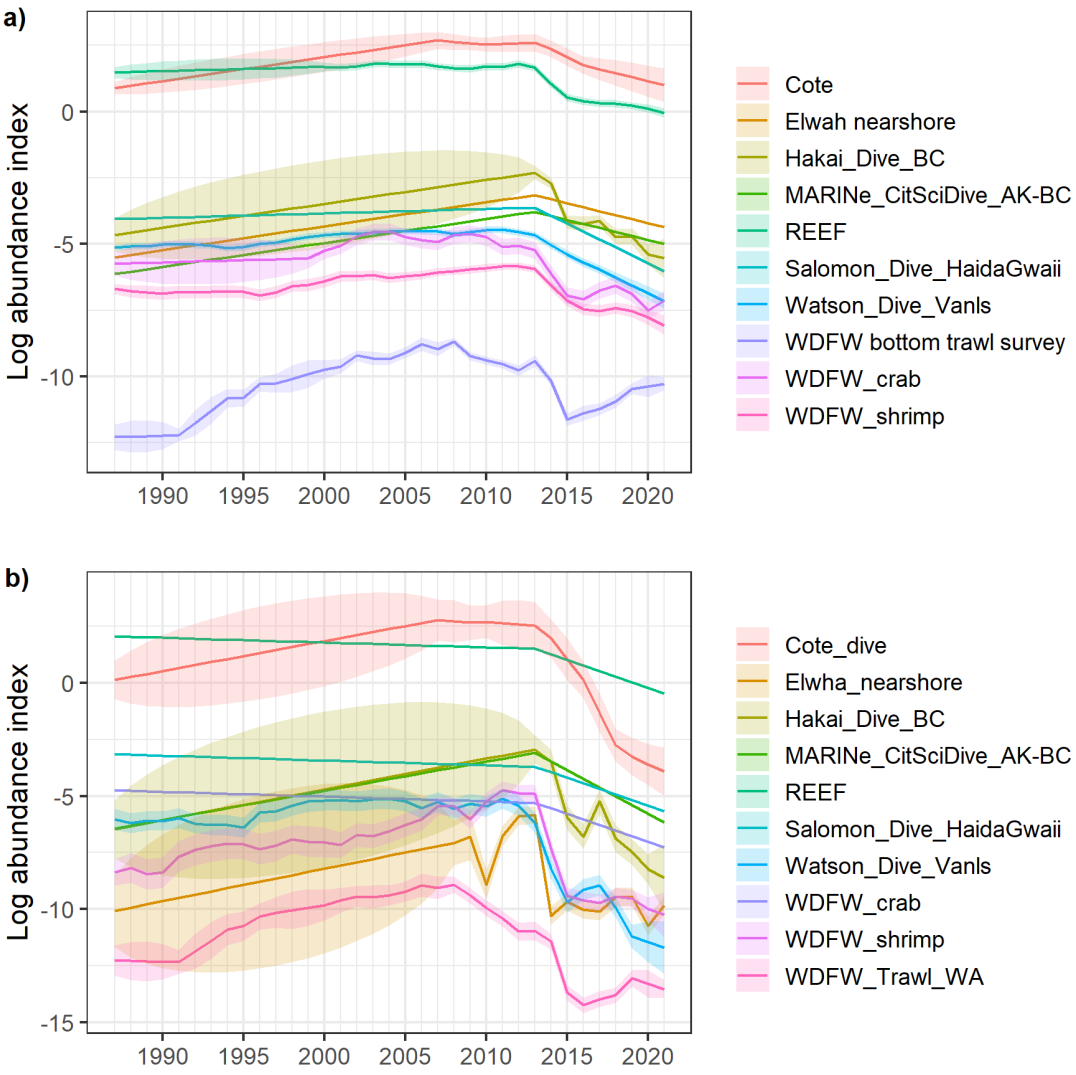


**Figure A4.2.** Log abundance index of *P. helianthoides* in British Columbia and the Salish Sea from 1987-2021 based on MARSS analysis. a) results from the best-fit model with zeros replaced by NAs; b) results from the model with zeros replaced by a minimum value. Error envelopes indicate one standard error. Note, the inflated errors in some time series (pre-1999) occur because there are no data for that time series in that time period.

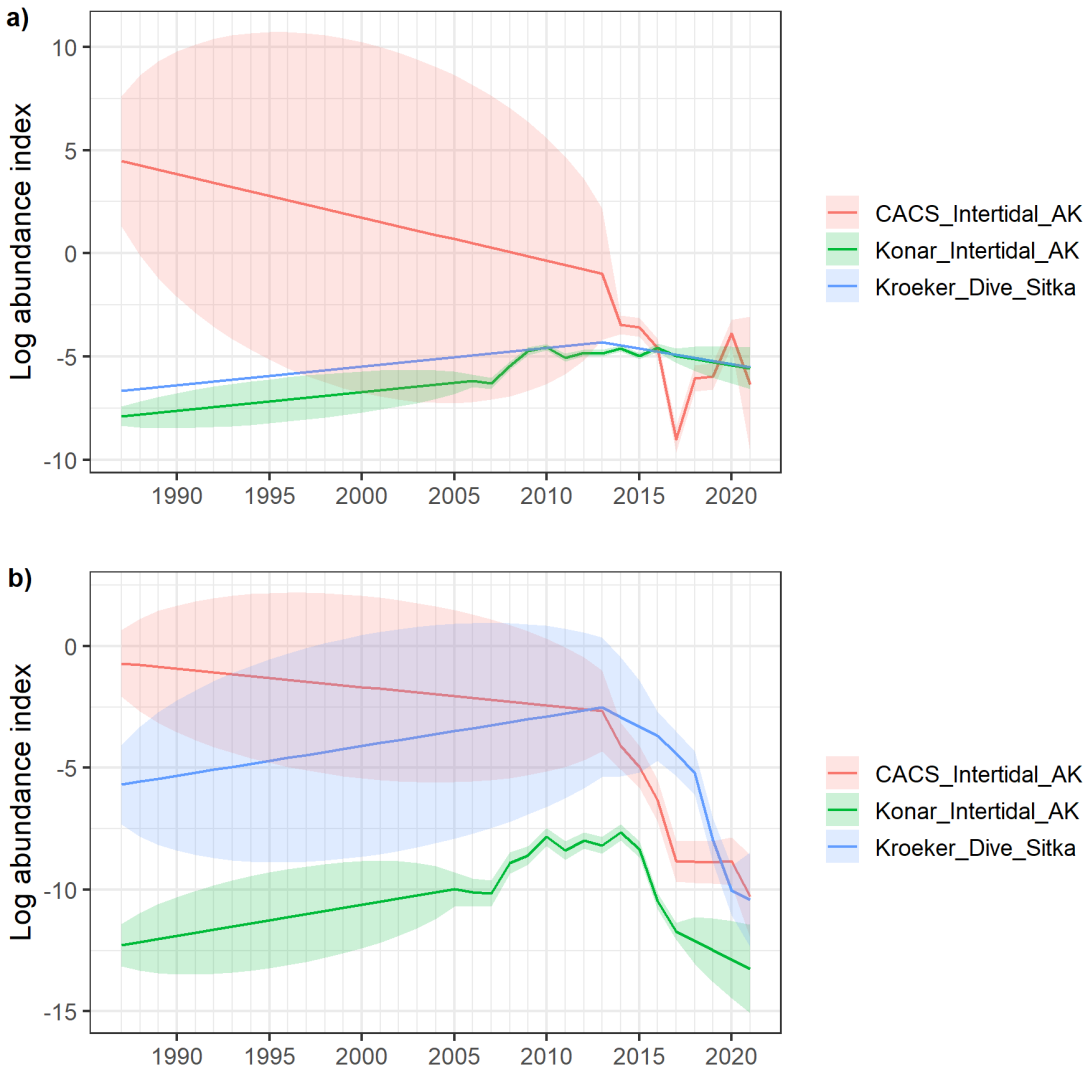


**Figure A4.3.** Log abundance index of *P. helianthoides* in Alaska from 1987-2021 based on MARSS analysis. Error envelopes indicate one standard error. a) results from the best-fit model with zeros replaced by NAs; b) results from the model with zeros replaced by a minimum value. Error envelopes indicate one standard error. Note, the inflated errors in some time series (pre-1999) occur because there are no data for that time series in that time period.

### A4.6.3 Region-specific model runs

The negative rate of population growth for *P. helianthoides* in Alaska prior to 2013 did not appear to match the actual time series data and was largely driven by one source (CACS_intertidal_AK), which contained no data in the pre-2013 period. Replacing zeros with minimum values reduced the rate of decline, but the results still failed to follow the only pre-2013 data available, Konar_Intertidal_AK, in which the estimated state increased prior to 2013 (Figure 4.3). Therefore, additional, targeted model runs were completed to address the negative estimate of population growth rate for the Alaska region from the best-fit model for the pre-2013 period but running a MARSS analysis using only the Alaska data, either with zeros replaced by NAs (Alaska-only w/NA) or with zeros replaced by the estimated minimum values (Alaska-only w/min). For completeness, similar MARSS models

were run for the combined British Columbia and Salish Sea region, and for the West Coast region. While the primary focus was on Alaska, these region-specific analyses are presented in the same order as above, progressing northward.

#### *A4.6.3.1 West Coast*

For the West Coast only (Figure A4.4), MARSS provided relatively consistent estimates of post-2013 rates of population decline (Table A4.4) at around -23.5% annually. However, the WC-only model suggested a higher rate of decline at -37.2%. West Coast-only w/min had several time series with exploding process variance, and these results should be interpreted cautiously (Figure A4.4). Three of the four models estimated a greater than 90% decline in population size in 2022 relative to 2013 (Table A4.5), with the fourth model estimating an 89.1% decrease.

**Table A4.4.** Selected model coefficients for the West Coast region from four models. Best-fit w/NA is Model 1 from the main model comparison exercise that included all regions, but only the results for Alaska are shown. Best-fit w/min has the same model structure, but the zeros in the data set were replaced with minimum values determined as 0.001 times the mean of the data source. The West Coast only models include only West Coast data with either zeros replaced by NAs or by the minimum values for each data source. U.t1 and U.t2 are population growth rates pre-2013 and post-2013, respectively, for each region as defined by Z. Q = process variance, R.diag = observation variance. The scaling factor A has been omitted. Standard errors were not calculated due to extensive run times.

| Parameter | Best-fit w/NA | Best-fit w/min | WC w/NA | WC w/min |
|---|---|---|---|---|
| U.t1-West Coast | 0.017 | -0.021 | 0.056 | 0.013 |
| U.t2-West Coast | -0.299 | -0.246 | -0.465 | -0.260 |
| Q.West Coast_CADFW_Dive_NorCal | 0.339 | 0.000 | 0.471 | 0.953 |
| Q.West Coast_CADFW_ROV_CA | 0.000 | 0.483 | 0.906 | 1.295 |
| Q.West Coast_COBI_Dive_Baja | 0.000 | 0.000 | 0.000 | 0.000 |
| Q.West Coast_MBNMS_Dive_BigSur | 0.000 | 0.000 | 0.000 | 0.000 |
| Q.West Coast_WCGBTS | 0.456 | 1.290 | 0.331 | 3,089,516.395 |
| Q.West Coast_OCNMS_Dive_Olympic | 0.000 | 14.957 | 0.000 | 289,979.733 |
| Q.West Coast_ODFW_Dive_OR | 0.111 | 4.961 | 0.000 | 4.905 |
| Q.West Coast_ODFW_ROV_OR | 1.122 | 1.697 | 0.997 | 1.650 |
| Q.West Coast_PISCO_Dive_CA | 0.059 | 0.832 | 0.046 | 0.818 |
| Q.West Coast_ReefCheck_Dive_CA | 0.126 | 0.778 | 0.046 | 3,509,588.421 |
| Q.West Coast_REEF | 0.000 | 0.000 | 0.000 | 0.000 |
| Q.West Coast_Williams_dive | 0.000 | 0.000 | 0.000 | 0.000 |
| R.diag | 0.431 | 2.816 | 0.463 | 2.892 |

**Table A4.5.** Summarized estimates of population growth rate for the West Coast region from four models.

| Model | U1 | Pre-2013 annual % | U2 | Post-2013 annual % | % decline since 2013 |
|---|---|---|---|---|---|
| Best-fit w/NA | 0.017 | 1.7 | -0.299 | -25.8 | 93.2 |
| Best-fit w/min | -0.021 | -2.1 | -0.246 | -21.8 | 89.1 |
| WC w/NA | 0.056 | 5.8 | -0.465 | -37.2 | 98.5 |
| WC w/min | 0.013 | 1.3 | -0.260 | -22.9 | 90.3 |

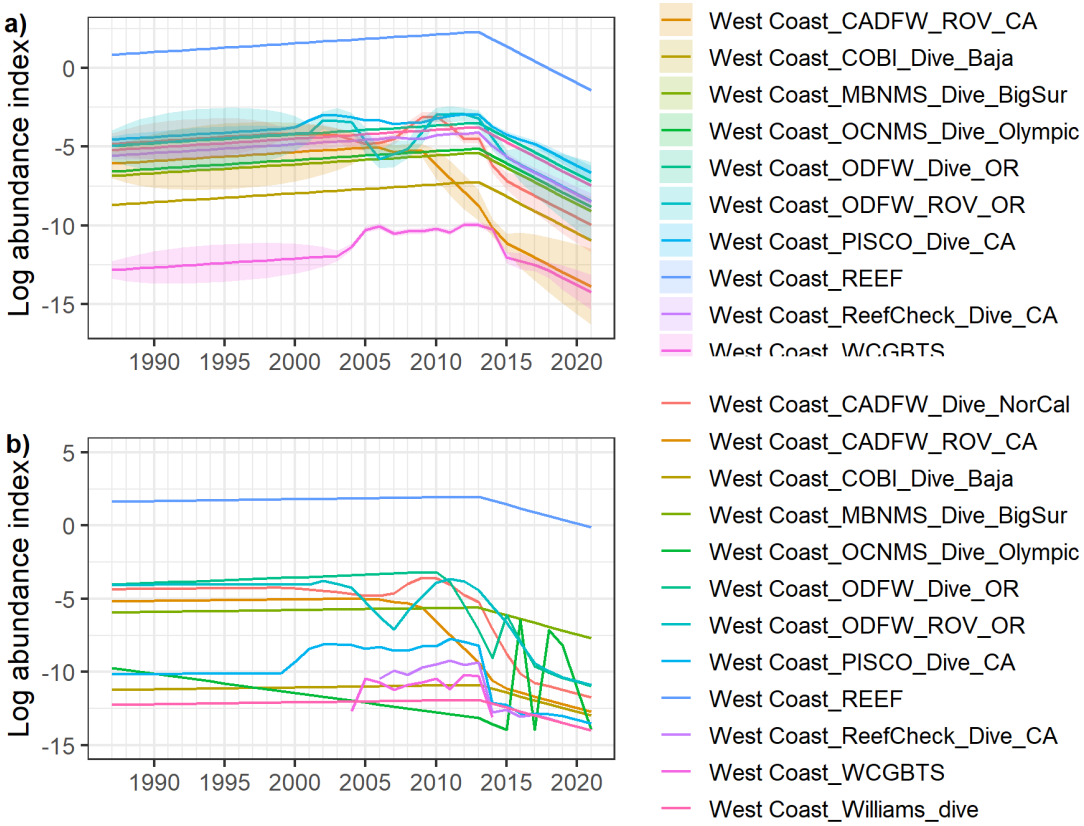


**Figure A4.4.** Log abundance index of *P. helianthoides* abundance on the West Coast from 1987-2021 based on MARSS analysis using only West Coast data. Error envelopes indicate one standard error. a) results from the model with zeros replaced by NAs; b) results from the model with zeros replaced by a minimum value. Error envelopes indicate one standard error. Note, the inflated errors in some time series (pre-1999) occur because there are no data for that time series in that time period. Error envelopes are not plotted in (b) because they are extremely large.

### *A4.6.3.2 British Columbia and Salish Sea*

For the combined British Columbia and Salish Sea region, population growth rate $u$ from 2013 onwards was fairly similar for the full models including all regions (best-fit w/NA or best-fit w/min) versus the BC-only models (Table A4.6, Figure A4.5). The models using minimum values for zeros did estimate greater rates of decline post-2013. Process variance for the BC-only w/NA exploded for three of the time series, and results for this model should certainly be taken with caution. As with Alaska, observational variance was higher

for the minimum value models than for the w/NA models resulting in extremely high standard errors and low confidence in the model.

**Table A4.6.** Selected model coefficients for the combined British Columbia and Salish Sea region from four models. Best-fit w/NA is Model 1 from the main model comparison exercise that included all regions, but only the results for the British Columbia and Salish Sea region are shown. Best-fit w/min has the same model structure, but the zeros in the data set were replaced with minimum values determined as 0.001 times the mean of the data source. The BC only models include only British Columbia and the Salish Sea region; data are with either zeros replaced by NAs or by the minimum values for each data source. U.t1 and U.t2 are population growth rates pre-2013 and post-2013, respectively, for each region as defined by Z. Q = process variance, R.diag = observation variance. The scaling factor A has been omitted. Parameter standard errors were calculated for the BC-only models.

| Parameter | Best-fit w/NA | Best-fit w/min | BC only w/NA | se | BC only w/min | se |
|---|---|---|---|---|---|---|
| U.t1 | 0.090 | 0.129 | 0.005 | 0.034 | -0.017 | 76.438 |
| U.t2 | -0.151 | -0.384 | -0.142 | 0.038 | -0.271 | 201.545 |
| Q.BC and Salish Sea_Cote_dive | 0.059 | 0.767 | 64,708.710 | 85,738.688 | 0.950 | 134,678.506 |
| Q.BC and Salish Sea_Elwha_nearshore | 0.000 | 2.663 | 0.000 | 0.011 | 2.879 | 944,734.926 |
| Q.BC and Salish Sea_Hakai_Dive_BC | 0.399 | 1.738 | 0.455 | 0.295 | 2.058 | 417,885.392 |
| Q.BC and Salish Sea_MARINe_CitSciDive_AK-BC | 0.000 | 0.000 | 51,604.241 | 42,328.274 | 0.000 | 902,325.468 |
| Q.BC and Salish Sea_REEF | 0.045 | 0.000 | 0.041 | 0.026 | 0.000 | 414,113.160 |
| Q.BC and Salish Sea_Salomon_Dive_HaidaGwaii | 0.000 | 0.000 | 0.000 | 0.021 | 0.000 | 652,148.574 |
| Q.BC and Salish Sea_WDFW_Trawl_WA | 0.283 | 0.551 | 304,156.983 | 180,780.385 | 0.563 | 1,340,907.333 |
| Q.BC and Salish Sea_WDFW_shrimp | 0.057 | 0.695 | 0.096 | 0.052 | 0.702 | 984,446.933 |
| Q.BC and Salish Sea_WDFW_crab | 0.225 | 0.000 | 0.284 | 0.148 | 0.000 | 729,074.099 |
| Q.BC and Salish Sea_Watson_Dive_VanIs | 0.016 | 0.539 | 0.056 | 0.031 | 0.574 | 234,257.771 |
| R.diag | 0.431 | 2.816 | 0.355 | 0.018 | 2.513 | 1,387.860 |

Estimates of total population decline were greater than 70% for the NA models and greater than 90% for the models with zeros replaced by minimum values (Table AA4.7). Three of the four models found increasing population size prior to 2013.

**Table A4.7.** Summarized estimates of population growth rate for the British Columbia and Salish Sea region from four models.

| Model | U1 | Pre-2013 annual % | U2 | Post-2013 annual % | % decline since 2013 |
|---|---|---|---|---|---|
| Best-fit w/NA | 0.090 | 9.4 | -0.151 | -14.1 | 74.4 |
| Best-fit w/min | 0.129 | 13.8 | -0.384 | -31.9 | 96.8 |
| BC only w/NA | 0.005 | 0.5 | -0.142 | -13.2 | 72.0 |
| BC only w/min | -0.017 | -1.7 | -0.271 | -23.7 | 91.3 |

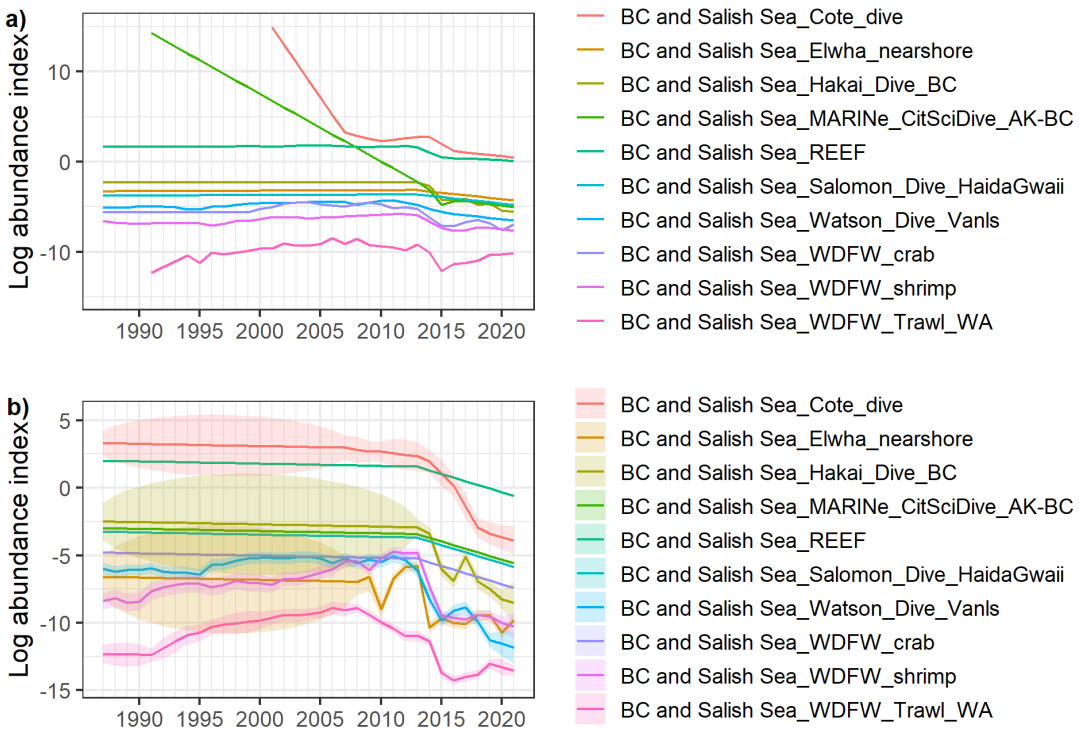


**Figure A4.5.** Log abundance index of *P. helianthoides* abundance in British Columbia and the Salish Sea from 1987-2021 based on MARSS analysis using only British Columbia and the Salish Sea data. Error envelopes indicate one standard error. a) results from the model with zeros replaced by NAs; b) results from the model with zeros replaced by a minimum value. Error envelopes indicate one standard error. Note, the inflated errors in some time series (pre-1999) occur because there are no data for that time series in that time period. Error envelopes are not plotted in a) because they are extremely large.

### *A4.6.3.3 Alaska*

When the Alaska data were analyzed alone, the rate of population growth pre-2013 was positive for both w/NA (23% per year) (Figure A4.6), and w/min model (15% per year) (Table A4.8). Estimates of $u_{post2013}$ for differed widely among the four models. Additionally, replacing zeros with minimum values shifted variance from process variance in the NA models to observational variance in the /min, and in the Alaska-only model with minimum values, MARSS was unable to estimate process variance.

Three of the four models predicted and almost complete extirpation of *P. helianthoides* with population size in 2022 decreasing by greater than 99% compared to 2013 (Table A4.9). Only the Alaska-only w/NAs predicted less decline with population size having decreased by 80.6% since 2013.

**Table A4.8.** Selected model coefficients for the Alaska region from four models. Best-fit w/NA is Model 1 from the main model comparison exercise that included all regions, but only the results for Alaska are shown. Best-fit w/min has the same model structure, but the zeros in the data set were replaced with minimum values determined as 0.001 x the mean of the data source. The Alaska only models include only Alaska data with either zeros replaced by NAs or by the minimum values for each data source. U.t1 and U.t2 are population growth rates pre-2013 and post-2013, respectively, for each region as defined by Z. Q = process variance, R.diag = observation variance. The scaling factor A has been omitted. Parameter standard errors were calculated for the Alaska-only models.

| Parameter | Best-fit w/NA | Best-fit w/min | AK only w/NA | se | AK only w/min | se |
|---|---|---|---|---|---|---|
| U.t1 | -0.210 | -0.069 | 0.207 | 0.141 | 0.374 | 0.082 |
| U.t2 | -2.475 | -1.447 | -0.182 | 0.241 | -1.017 | 0.128 |
| Q.Alaska_CACS_Intertidal_AK | 10.295 | 1.970 | 3.767 | 2.096 | 0.000 | 0.046 |
| Q.Alaska_Konar_Intertidal_AK | 0.226 | 0.791 | 0.133 | 0.138 | 0.000 | 0.005 |
| Q.Alaska_Kroeker_Dive_Sitka | 0.000 | 2.739 | 0.000 | 0.221 | 0.000 | 0.056 |
| R.diag | 0.431 | 2.816 | 0.620 | 0.087 | 3.901 | 0.390 |

**Table A4.9.** Summarized estimates of population growth rate for the Alaska region from four models.

| Model | U1 | Pre-2013 annual % | U2 | Post-2013 annual % | % decline since 2013 |
|---|---|---|---|---|---|
| Best-fit w/NA | -0.210 | -19.0 | -2.475 | -91.6 | 100.0 |
| Best-fit w/min | -0.069 | -6.6 | -1.447 | -76.5 | 100.0 |
| AK only w/NA | 0.207 | 23.0 | -0.182 | -16.7 | 80.6 |
| AK only w/min | 0.374 | 45.3 | -1.017 | -63.8 | 100.0 |

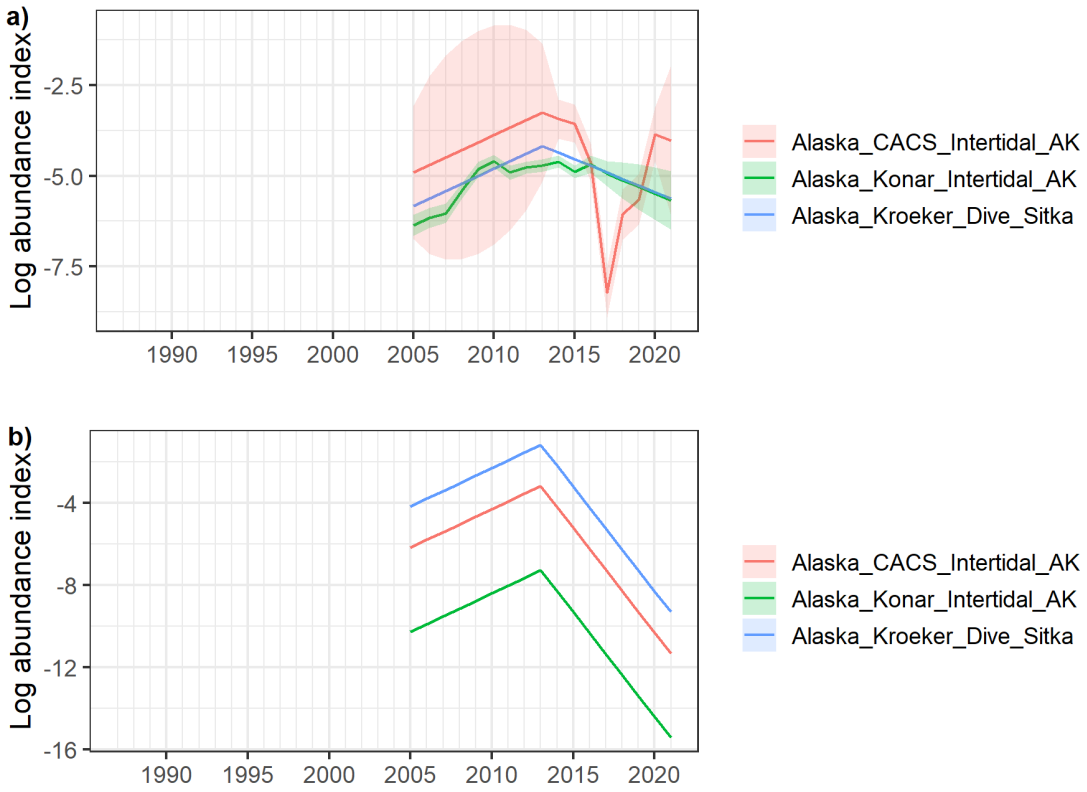


**Figure A4.6.** Log abundance index of *P. helianthoides* abundance in Alaska from 2005-2021 based on MARSS analysis using only Alaska data. Error envelopes indicate one standard error. a) results from the model with zeros replaced by NAs; b) results from the model with zeros replaced by a minimum value. Error envelopes indicate one standard error. Note, the inflated errors in some time series (pre-1999) occur because there are no data for that time series in that time period.

## A4.7 Extinction risk

Estimating both population growth rate $u$ and the process variance $Q$ allows for the estimation of extinction risk (Holmes et al. 2021). In practice, one does not estimate the risk of reaching a population size of zero, but instead the risk of the population size dropping below some threshold value. Here the threshold value ($p_d$) for extinction risk was set at 1% of 2013 value and calculated as $p_d = 0.01/exp(u)^{(2022-2013)}$. Extinction risk, then, was assessed as the probability of *P. helianthoides* population dropping below 1% of its 2013 population size over a 30-year future time-horizon. In some MARSS output, $N_{2022}$ is already estimated to be below this value.

Of course, using post-2013 estimates of $u$ assumes that growth rate remains negative into the future because of continuing SSWS impacts, and potentially Alee effects. Under these conditions, the risk of declining below 1% of the 2013 population size is essentially 100% and the only question is how quickly that threshold is reached. An alternative scenario is that the effects of SSWS abate, Alee effects are negligible, and *P. helianthoides* populations begin to grow at annual rates seen prior to 2013. Both scenarios are presented here for each region for all four models by estimating extinction risk based on both the pre-2013 and post-2013 estimates of $u$ for each region.

The probability of dropping below the 1% threshold was calculated following Dennis et al. (1991):

$$\Pi(x_d, t_e) = \pi(u) * \Phi\left(\frac{-x_d + |u|t_e}{\sqrt{\sigma^2 t_e}}\right) + exp(2x_d|u|/\sigma^2)\Phi\left(\frac{-x_d - |u|t_e}{\sqrt{\sigma^2 t_e}}\right)$$

where $\Phi(x_d, t_e)$ is the probability that the population will hit a threshold $x_d$ (0.01) over the time horizon of $t_e$=30 years. A fractional decline was estimated such that:

$$x_e = log(N_0/p_d * N_0) = -log(p_d).\pi(u)$$

were $x_e is$ the threshold, $N_0$ is the current population estimate, $p_d$ is the threshold (here 0.01), and $\pi(u)$ is the probability of eventually dropping below the threshold by $t_e = \infty$. $\Phi(\quad)$ is the cumulative standard normal probability distribution with mean=0 and sd=1. The term $u$ is the same rate of population growth/decline as in the MARSS parameterization, while $\sigma^2$ is the process variance $Q$ from the MARSS analysis.

Note that the results for the combined British Columbia and Salish Sea region align most closely with the region identified as British Columbia in the significant portion of its range analysis (section 6.5.2).

### A4.7.1 West Coast

For the West Coast, the post-2013 rates of population decline all predicted high risk that *P. helianthoides* populations would drop below 1% of population size in 2013 with all models exceeding 90% within the 30-year horizon (Figure A4.7). This is hardly surprising given that the post-2013 growth rates are uniformly negative and predict a continued decline. If population growth returns to pre-2013 levels, the probability of extinction is predicted to be low for two of the scenarios, although the best-fit w/min model did predict continued decline and a greater than 50% chance of dropping below 1% of the 2013 population size. However, this negative $u$ does not represent a potential recovery scenario. The West Coast only w/min was excluded from the extinction risk analysis due to extreme estimates of process variance.

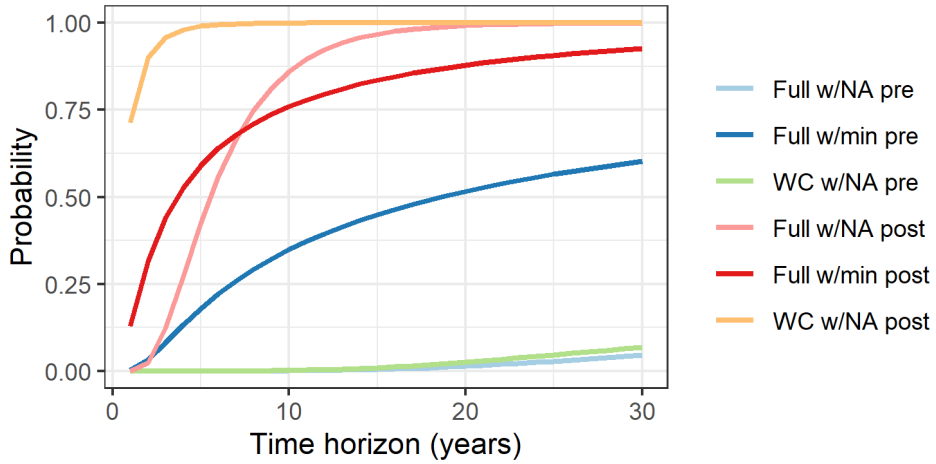


**Figure A4.7.** Extinction risk for *P. helianthoides* in the West Coast region from four models. The Full models the best-fit model with zeros replaced by NAs or minimum values. The WC-only models include only the time series from the West Coast. Estimates are presented using either the pre-2013 or post-2013 population growth rate. The risk is the probability that the population size will drop below a threshold 1% of its value in 2013.

### A4.7.2 British Columbia and the Salish Sea

The BC-only w/NA model was not included in the extinction risk calculations for the combined British Columbia and Salish Sea region because prior evaluation identified ballooning process variance in several terms.

All three included scenarios using post-2013 population growth rates suggested a high probability that *P. helianthoides* population size would drop below 1% relative to 2013 within the 30-year time frame (Figure A4.8). The least pessimistic post-2103 $u$ model, the full model with NAs, predicted that risk would reach 80% within 30 years. None of the models using the pre-2013 growth rates suggested high extinction risk.

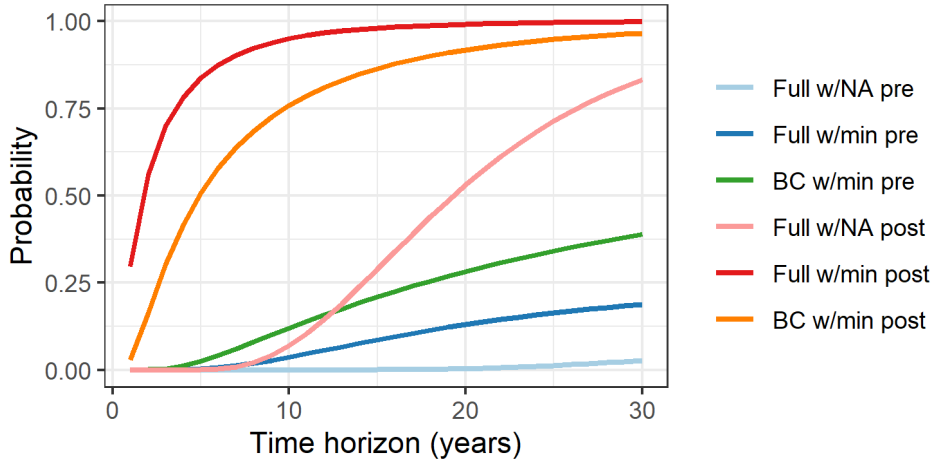


**Figure A4.8.** Extinction risk for *P. helianthoides* in the combined British Columbia and Salish Sea region from four models. The Full models the best-fit model with zeros replaced by NAs or minimum values. The BC-only models include only the time series from British Columbia and the Salish Sea. Estimates are presented using either the pre-2013 or post-2013 population growth rate. The risk is the probability that the population size will drop below a threshold 1% of its value in 2013.

### A4.7.3 Alaska

Estimates of population growth from the two full models with all three major regions (best-fit w/NA and best-fit w/min) were not included in the extinction risk calculations for the Alaska region since previous evaluation identified problems with the pre-2013 estimates for $u$. Additionally, the extinction risk for the Alaska-only w/min model was not included because this model was unable to estimate process variance (Table A4.8), which is necessary for the calculations.

Assuming post-2013 population growth rates, three of the four estimates of population decline for Alaska exceeded 99% (Table AA4.7). For these scenarios the extinction risk already exceeds the 1% threshold and the results overlap in Figure A4.9 at 1.0. AK-only w/NA predicted an 80.6% decline since 2013 at -16.7% per year. For this model, extinction risk reached 86% in 30 years. For the Alaska-only w/NA model, risk remained below 25% over the next 30 years.

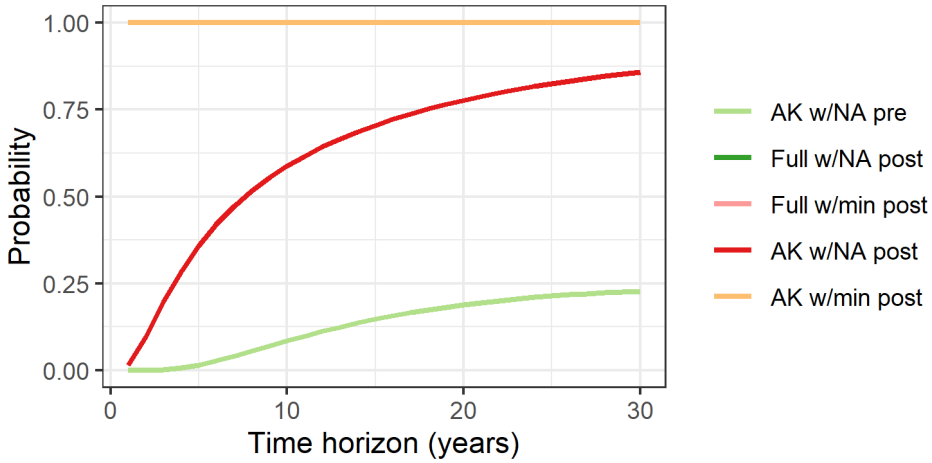


**Figure A4.9.** Extinction risk for *P. helianthoides* in the Alaska region from four models. The Full models the best-fit model with zeros replaced by NAs or minimum values. The AK only models include only the AK data. Estimates are presented using either the pre-2013 or post-2013 population growth rate. The risk is the probability that the population size will drop below a threshold 1% of its value in 2013.

## A4.8 Discussion

The question of whether SSWS ceases to have strong impacts on *P. helianthoides* population growth rates is central to evaluating the actual risk of extinction. All of the models here suggest the risk is high that *P. helianthoides* populations will drop below 1% of their 2013 sizes if SSWS does not abate and population growth continues to be negative; this result is hardly surprising given the projected continued population decline from assuming post-2013 rates of change.

Should SSWS abate, and in the absence of strong Alee effects, *P. helianthoides* appear likely to recover if population growth rates return to pre-2013 levels. Moreover, *P. helianthoides* are likely similar to other echinoderms, which have boom-bust population dynamics, and recovery could occur quickly under the right conditions. However, the time series show little to any signs of recovery, suggesting that post-2013 population declines may continue

into the foreseeable future. The exception is the REEF data for the Salish Sea, which show a small, persistent increase for the Canadian waters and observations remaining above zero in the US portion of the Salish Sea (Figure A3.23). Most other time series remained at zero individuals post-crash with no sign of recovery.

Hamilton et al. (2021) report some recruitment in the Gulf of Alaska and British Columbia, but note that these individuals fail to persist to adults, likely because of ongoing impacts of SSWS. Several of the time series here did show minor, but ephemeral, increases in *P. helianthoides* abundance after the ~2013 die-off. For example, the Watson dive date for Vancouver Island and the WDFW shrimp test fishery both show short-lived increases. Clearly understanding whether SSWS will persist and continue to kill off recruitment pulses is key to understanding future *P. helianthoides* population dynamics on a regional and global basis.

The three major analyses of *P. helianthoides* population status, Hamilton et al. (2021), Gravem et al. (2021), and the MARSS analysis here, all generally agree on substantial declines in abundance across the species' range (Table A4.10). In part, one should expect this result given that all three analyses use similar data sets. Declines were strongest in the southern portion of the species range (here West Coast region). However, the results are somewhat more variable for Alaska ranging from 40-100% for Hamilton et al. (2021) and 61%-95% for Gravem et al. (2021) across various Alaskan regions. MARSS estimates of decline in Alaska since 2013 ranged from 81-100% depending on whether zeros were replaced with NAs or minimum values, with w/NA models estimating smaller declines.

The combined British Columbia and Salish Sea region match most closely with the core region from the significant portion of its range analysis (section 6.5.2). Here MARSS estimated an average 84% decline across models, ranging from 72-96%. Both Hamilton et al. (2021) and Gravem et al. (2021) estimated declines around 88% for British Columbia, although their estimates for the Salish Sea suggested higher loss. While there is some variation among modeling approaches and studies, the extinction risk analysis here (the probability that population size drops below 1% of the 2013 population size over the next 30 years) is high if population growth rate continues to be negative, but much lower if *P. helianthoides* population growth returns to pre-2013 levels.

**Table A4.10.** Change in density and occurrence after the onset of SSWS through 2020 from Hamilton et al. (2021) and Gravem et al. (2021), and through 2021 for the MARSS analyses here. Summarized results from the MARSS analysis are shown in the two right columns. The MARSS % decline is the mean across all models for that region. The range shows the range of estimated decline.

| Hamilton regions | % decline in density | Gravem regions | % decline in density | MARSS Region | Mean MARSS % decline | MARSS % range |
|---|---|---|---|---|---|---|
| Aleutians | 40.0 | Aleutians | | | | |
| West Gulf of Alaska | 100.0 | West Alaska | 61.1 | Alaska | 95.2 | 80.6-100 |
| East Gulf of Alaska | 93.8 | East Gulf of Alaska | 94.9 | | | |
| Southeast Alaska | 96.0 | Southeast Alaska | 94.7 | | | |
| British Columbia | 87.9 | British Columbia | 87.9 | BC & SS | 83.6 | 72-96.8 |
| Salish Sea | 92.4 | Salish Sea | 91.9 | | | |
| Washington coast | 99.6 | Coastal PNW | 99.6 | West Coast | 92.8 | 89.1-98.5 |
| Oregon | 100.0 | | | | | |
| Northern California | 99.2 | Northern California | 97.9 | | | |
| Central California | 99.5 | Central California | 97.2 | | | |
| Southern California | 100.0 | Southern California | 99.8 | | | |
| Baja California | 100.0 | Baja California | 98.5 | | | |

## A5 Literature cited


Burnham KP, Anderson DR. (1998) Model selection and inference: a practical information-theoretic approach. Springer-Verlag, New York, NY.

Dennis B, Munholland PL, Scott JM. (1991) Estimation of growth and extinction parameters for endangered species. Ecological Monographs 61:115-143.

Gravem SA, Heady WN, Saccomanno VR, Alvstad KF, Gehman ALM, Frierson TN, Hamilton SL. (2021) IUCN Red List: Sunflower Sea Star (*Pycnopodia helianthoides*). IUCN Red List of threatened species 2021.

Hamilton SL, Saccomanno VR, Heady WN, Gehman AL, Lonhart SI, Beas-Luna R, Francis FT, Lee L, Rogers-Bennett L, Salomon AK, Gravem SA. (2021) Disease-driven mass mortality event leads to widespread extirpation and variable recovery potential of a marine predator across the eastern Pacific. Proceedings of the Royal Society B-Biological Sciences 288.

Harvey CJ, Garfield T, Williams G, Tolimieri N (eds). (2022) 2021-2022 California Current ecosystem status report: A report of the NOAA California Current Integrated Ecosystem Assessment Team (CCIEA) to the Pacific Fishery Management Council, March 13, 2022.

Holmes EE, Ward EJ, Scheuerell MD. (2021) Analysis of multivariate time-series using the MARSS package, version 3.11.4. NOAA Fisheries, Northwest Fisheries Science Center, 2725 Montlake Blvd E., Seattle, WA 98112.

Holmes EE, Ward EJ, Wills K. (2012) MARSS: Multivariate autoregressive state-space models for analyzing time-series data. The R Journal 4:11-19.

Keller AA, Wallace JR, Methot RD. (2017) The Northwest Fisheries Science Center's West coast groundfish bottom trawl survey: History design, and description. NOAA Technical Memorandum NMFS NWFSC, Book 136. U.S. Department of Commerce.

Lekanda A, Tolimieri N, Nogueira A. (2021) The effects of bottom temperature and fishing on the structure and composition of an exploited demersal fish assemblage in West Greenland. ICES Journal of Marine Science 78:2895-2906.
REEF. (2022) Reef Environmental Education Foundation. World Wide Web electronic publication www.reef.org.
Tolimieri N, Holmes EE, Williams GD, Pacunski R, Lowry D. (2017) Population assessment using multivariate time-series analysis: A case study of rockfishes in Puget Sound. Ecology and Evolution 7:2846-2860.